



Holocene environmental changes in the Fuegian forest and steppe, Argentina



Andrea Coronato^{a,b,*}, Ana María Borromei^c, Juan Federico Ponce^{a,b}, Soledad Candel^{a,d}, Lorena Musotto^c, Marilén Fernández^a, Cecilia Laprida^e, Adriana Mehl^f, Alejandro Montes^{a,b}, Cristina San Martín^{a,b}, Adolfinia Savoretti^{a,b}, Gabriela Cusminsky^g, Sandra Gordillo^h, María Julia Orgeiraⁱ, Ramiro López^a, Pamela Alli^{a,d}, Diego Quiroga^{a,b}

^a CONICET-CADIC, B. Houssay 200, V9410BWB, Ushuaia, Argentina

^b ICPA-UNTDf, Walanika 250, V9410BWB Ushuaia, Argentina

^c CONICET-UNS-INGEoSUR, Avenida Alem, 1253, Cuerpo B', Piso 2°, B8000CPB, Bahía Blanca, Argentina

^d IDEI-UNTDf, Walanika 250, V9410BWB, Ushuaia, Argentina

^e CONICET-UBA-IDEAN, Intendente Güiraldes 2160 - Pabellón II, Piso 2, Ciudad Universitaria, C1428EGA, Ciudad Autónoma de Buenos Aires, Argentina

^f CONICET-INCITAP, Uruguay 151, L6300CLB Santa Rosa, Argentina

^g CONICET-UNCOMA-INIBIOMA, Quintral 1250, 8400 San Carlos de Bariloche, Argentina

^h CONICET-UNCo-IDACOR, Avda. Hipólito Yrigoyen 174, X5000JHO Córdoba, Argentina

ⁱ CONICET-UBA-IGEBA, Intendente Güiraldes 2160, Pabellón II, Piso 1, Ciudad Universitaria, C1428EGA, Ciudad Autónoma de Buenos Aires, Argentina

ARTICLE INFO

Keywords:

Late Quaternary
Southern Patagonia
Environmental variability
Southern hemisphere westerlies
Terrestrial and marine environments

ABSTRACT

Environmental changes were reconstructed from a multiproxy synthesis of over 30 localities from the Isla Grande de Tierra del Fuego and Isla de los Estados, southernmost South America. At a local scale, the results from the mountain forest and gently undulating steppe areas were integrated as well as those from the marine environments of the Beagle Channel and the Atlantic coasts. At a regional scale, the results were integrated with those published for the southernmost Andean and Extra-Andean Patagonia and the Antarctic Peninsula. This study focuses on the environmental evolution during the Late Glacial-Holocene transition, the Middle to Late Holocene transgressive-regressive hemicycle and wet-dry oscillations, the Medieval Climate Anomaly, the Little Ice Age, the tephra inputs from the Patagonian Andes, and the recent climatic warming. Most paleoenvironmental changes are related to variations in the latitudinal position and intensity of the Southern Westerly Winds (SWW) while others are associated with astronomical or endogenous forcings. At a strong intensity of the SWW, a greater contribution of humidity to the forest areas and an increase in the rainfall gradient create windy and arid conditions in the steppe. At a weak intensity of the SWW, lower humidity input in the forest areas and the advection of air masses from the Atlantic Ocean promoted humid and slightly windy conditions in the steppe. Similar environmental trends are observed between terrestrial and marine environments in the center and south of Tierra del Fuego, Isla de los Estados and the Antarctic Peninsula, and between the Fuegian steppe and Extra-Andean Patagonia. The paleoclimatic evidence reveal high environmental variability in the last 10,000 years for this sector of the Southern Hemisphere.

1. Introduction

At the southern tip of South America, the Fuegian Archipelago extends as a landmass at sub-Antarctic latitudes. The Isla Grande de Tierra del Fuego (IGTDF, Fig. 1 A) is the largest island in the Fuegian Archipelago. The Isla de los Estados (IDE, Fig. 1 A), located to the east of

Tierra del Fuego is a projection of the Fuegian Andes and the *Nothofagus* forest. This island extends toward the Antarctic convergence as the Southern Hemisphere landmass emerging at sub-Antarctic latitudes. The climate is determined by its geographical location, the proximity to the Antarctic Circumpolar Current, the interplay between the Antarctic Polar Front and the Southern Westerly Winds (SWW) and conditioned by

* Corresponding author. CONICET-CADIC, B. Houssay 200, V9410BWB, Ushuaia, Argentina.

E-mail address: andrea.coronato@conicet.gov.ar (A. Coronato).

its physiography. As such, the Fuegian Archipelago is an exceptional place for the record of past regional and global environmental changes in sub-Antarctic terrestrial environments since those variables confer an exceptional characteristic to the atmospheric and geodynamic processes of the area.

Reconstructions of the last 10,000 years have revealed high variability in the processes on the earth's surface and the Fuegian Archipelago. These processes were affected by astronomical factors linked to changes in insolation (Renssen et al., 2005; Berman et al., 2018), or endogenous factors linked to glacio-isostasy, tectonics, and volcanism (Stern, 2008; Wastegård et al., 2013; Reynhout et al., 2019, among others). Some internal forcings operating within the climate system are, i.e., changes, in the position of the South Pacific semipermanent anticyclone (Kilian and Lamy, 2012; Moreno et al., 2018, among others), or hydrometeorological changes that generate relative variations in lake levels (Ariztegui et al., 2008; Horta et al., 2011), or combination of these factors, reflected in changes in the mean sea level (Bujalesky, 2007; Bujalesky et al., 2021). Several authors have proposed that the dynamics of SWW are the main cause of the environmental changes in southern Patagonia, the Beagle Channel (BC), and the Antarctic Peninsula (AP) (Schäbitz et al., 2013; Moreno et al., 2018; McCulloch et al., 2020, among others), in oceanic environments outside the region but affected by the SWW belt (Perren et al., 2020), or changes in the oceanic circulation (Waelbroeck et al., 2011).

This article analyzes several sites and environments of the Argentinian sector of IGTDF and IDE, previously studied by the authors, with a multiproxy approach and discusses environmental changes that can be

attributed to glacio-isostasy, volcanism, astronomical variations, and solar cycles. These changes have been recorded in the sedimentary composition and fossil assemblages of terrestrial and marine environments, and in peat bogs, the typical Fuegian wetlands. Besides, regional volcanic events are recorded in aquatic and terrestrial sedimentary archives that reveal ecosystem shifts. On the global and regional scales, the two most representative physiographic units of IGTDF, the low mountain ranges and steppe plains in the north and the wooded mountains in the south, were affected by the same atmospheric processes but responded differently in their physical and biological components at the sub-regional and local scales. The postglacial transgressive-regressive hemicycle resulted in changes in paleocommunities and in various landforms and deposits in the BC and the Atlantic coast. This study aimed to analyze and compare the Holocene environmental changes recognized in the Fuegian steppe and forest regions during the Holocene, to analyze the influence of SWW in both regions, and to correlate the changes according to their chronologies and those available for southern Patagonia and the AP.

2. Methods

The results of our previous studies were integrated with those of classic studies. 35 sites distributed in the Argentinian sector of IGTDF and IDE that include Late Glacial, Holocene, and present time environmental changes are discussed. To determine the chronology and spatial structure of climate changes after the deglaciation, the studies were analyzed according to the analogous forest and steppe environments of

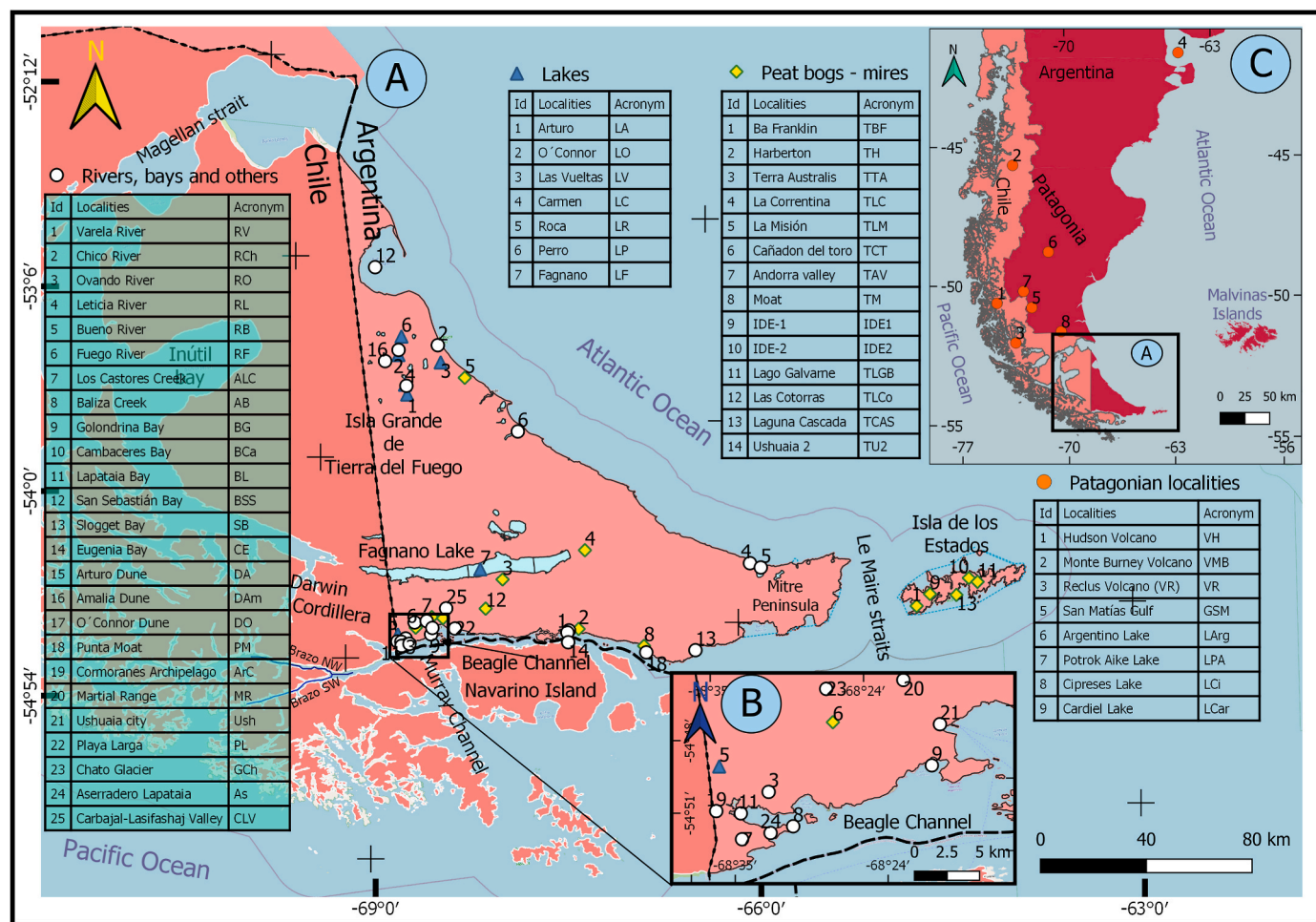


Fig. 1. Location maps. A) Isla Grande de Tierra del Fuego and Isla de los Estados. B) Western sector of the Beagle channel, from Ushuaia to Lapataia bays, at the southwest corner of the Beagle Channel (north coast). C) Southern Patagonia. The three maps show the localities and sampling sites mentioned in the text.

southern Patagonia and sub-Antarctic and Antarctic marine environments. The (sub) disciplines involved in this work include geomorphology, pedology, geochemistry, environmental geophysics, malacology and micropaleontology (palynomorphs, diatoms, ostracods, foraminiferal species, and plant macrofossils; see Table 1 for details). These varied set of disciplines involve also varied methodologies for sampling and dating. For instance, in modern micropaleontological studies sampling was performed at 1 cm in peat bogs and lacustrine cores, and at 2 cm intervals in sediment and paleosols outcrops, but in older one's sampling at 5–10 cm intervals were common. Dating also varied depending on objectives, material availability and other external factors; when it was possible, we considered dating at decadal or centennial resolution. Results coming from different proxies and disciplines enriched their interpretation and allowed us to reach conclusions about general patterns of the environmental changes that occurred in the two main regions of Tierra del Fuego.

Most of the previously obtained radiocarbon ages were calibrated by using Calib 8.20 software or previous versions considering the SHCal13 curve. When datings were published without calibration we calibrated to 1 and 2 σ using Calib 8.20 with SHCal20 (Hogg et al., 2020) and Marine 20 (Heaton et al., 2020) curves for continental and marine environments, respectively. All ages are referred to the median probability. In relation to the reservoir effect (ΔR) in marine shells and sediments, values of 221 ± 40 and 208 ± 66 years ^{14}C were considered for the BC based on Gordillo et al. (2015) and Björck et al. (2021). The regional age reservoir for marine records of the Antarctic Peninsula were considered as 1230 years by Etourneau et al. (2013) and 1000 years by Strelin et al. (2006).

The chronology of the events or processes analyzed follows the Holocene chronostratigraphic subdivision according to the International Commission on Stratigraphy of the International Union of Geological Sciences (IUGS). These are Early Holocene, between 11,700 and 8326 years before AD 2000; Mid Holocene, between 8326 and 4250 years before AD 2000; and Late Holocene, since 4250 years before AD 2000 (Walker et al., 2020; Aubry et al., 2020). Given that some geomorphological processes, environmental conditions, or proxy analyses started shortly before the Early Holocene, some aspects of the Late Glacial are also included in this study.

3. Study area

The Argentinian sector of IGTDF is located between $52^{\circ}39' - 55^{\circ}03'$ S and $65^{\circ}07' - 68^{\circ}36'$ W. The Magellan strait separates the island from the continental Patagonia to the north and partially from the Chilean Fuegian Archipelago to the west. Towards the south, the BC separates IGTDF and Chilean Fuegian Archipelago as the latter extends to the south. The South Atlantic Ocean and IDE lie to the east ($54^{\circ}42' - 54^{\circ}45'$ S and $63^{\circ}47' - 64^{\circ}45'$ W), the latter separated from IGTDF by the Lemaire strait (Fig. 1 A). The IGTDF comprises the Central Cordillera of the Fuegian Andes, extending in W-E direction, with a maximum elevation of ca. 1500 m a.m.s.l., and the Fuegian Thrust-Fold belt as its outer wedge, with a NW-SE direction, with a maximum elevation of ca. 900 m a.m.s.l. A transforming boundary between the South American and Scotia tectonic plates develops along the Magallanes-Fagnano Fault System, separating the orographic chains of the Fuegian Andes from the low hills. The geological history includes a submarine volcanic complex and Early Jurassic-Middle Cretaceous metasedimentary rocks (Olivero and Martinioni, 2001) affected by the Andean orogeny and deep marine sedimentary rocks grading beach deposits and continental environments to the north, folded in relation to provergent and retrovergent faults (Torres Carbonell et al., 2013), deposited and deformed throughout the Miocene.

At least five glaciations were recognized in the northern sector of Argentinian IGTDF over the last million years (Meglioli et al., 1990; Rabassa et al., 2000; Coronato et al., 2004; Díaz Balocchi et al., 2020; Quiroga et al., 2017), and at least the last two along the BC (Rabassa

Table 1

Disciplines and proxies applied to the study of the localities mentioned in the text and references of the corresponding main publications.

Localities	Code	Studied proxies and disciplines	References
North and central tierra del fuego (igtdf)			
SAN SEBASTIÁN BAY	BSS	Geomorphology, sedimentology, chronology.	Bujalesky (1997), 1998, 2007, Vilas et al., (1999)
CHICO RIVER	RCh	Geomorphology, sedimentology, chronology.	Montes, (2015) Bujalesky et al., (2021)
CARMEN LAKE	LC	Palynology (pollen/spores, algae), palynofacies, ostracods, diatoms, sedimentology, mineralogy, magnetic susceptibility, geochemistry.	Coronato et al., (2017) Villarreal and Coronato, (2017) Borromei et al. (2018) Laprida et al., (2021)
LAS VUELTAS LAKE	LLV	Geomorphology, sedimentology, palynology (pollen, non-pollen palynomorphs -NPPs-), diatoms, geochemistry, archaeology.	Montes et al., (2020) Candel et al., (2020)
O'CONNOR LAKE	LO	Geomorphology,	Bujalesky, (2007)
O'CONNOR DUNE	DO	geochemistry, pedology.	Villarreal and Coronato, (2017) Coronato et al., (2021)
ARTURO LAKE	LA	Geomorphology,	Montes et al., 2020
ARTURO DUNE	DA	environmental magnetism, chronology, diatoms, ostracods, organic matter content, pedology, palynology.	Coronato et al., (2011) Orgeira et al., (2012)
AMALIA DUNE	DAm	Geomorphology, pedology, Organic matter content, chronology.	Coronato et al., (2021)
FAGNANO LAKE	LF	Palynology, palynofacies, diatoms, geochemistry, sedimentology.	Waldmann et al., (2010) Waldmann et al., (2014)
LA CORRENTINA PEAT BOG	TLC	Palynology (pollen/spores, fungal remains), tephra analysis.	Musotto et al. (2016), 2017a
TERRA AUSTRALIS PEAT BOG	TTA	Palynology (pollen/spores, fungal remains), tephra analysis.	Musotto et al. (2017a), 2017b
SOUTH OF TIERRA DEL FUEGO (IGTDF)			
BAHÍA LAPATAIA	BL	Geomorphology, sedimentology, mollusks, palynology.	Gordillo et al., (1993) Borromei and Quattroccio, (2007) Rabassa et al., 2009a Gordillo et al., (2013) Candel et al., (2018)
ASERRADERO - LAPATAIA	AS	Geomorphology, sedimentology, mollusks, palynology (pollen/spores, algae).	Rabassa et al., 2009b Candel et al. (2009), 2018
ROCA LAKE	LRo	Geomorphology, mollusks, ostracods, foraminifera.	Rabassa et al., (1986) Gordillo et al., (1993)

(continued on next page)

Table 1 (continued)

Localities	Code	Studied proxies and disciplines	References
North and central tierra del fuego (igtdf)			
LOS CASTORES CREEK	ALC	Geomorphology, mollusks, ostracods, foraminifera.	Gordillo et al., (2013)
CORMORANES ARCHIPELAGO	ArC	Geomorphology, mollusks, ostracods, foraminifera.	Gordillo et al., (2013)
OVANDO RIVER	RO	Palynology, mollusks, ostracods, foraminifera.	Gordillo et al. (1993), 2013 Candel et al., (2009).
CAÑADÓN DEL TORO PEAT BOG	TCT	Palynology, sedimentology, geochemistry.	Borromei et al., (2016)
VALLE DE ANDORRA PEAT BOG	TVA	Palynology (pollen, fungal spores), testate amoebae, plant macrofossils.	Borromei (1995) Mauquoy et al., (2004)
BALIZA CREEK	AB	Geomorphology, sedimentology, palynology, mollusks.	Rabassa et al., 2009a Candel et al., (2017) Bernaconi et al. (2021)
GOLONDRINA BAY	BG	Foraminifera, ostracods, mollusks.	Gordillo et al., (2013)
PLAYA LARGA		Mollusks, geomorphology.	Gordillo et al. (1992)
USHUAIA 2 PEAT BOG	TU2	Palynology.	Heusser, (1998)
LAS COTORRAS PEAT BOG	TLC	Palynology (pollen, non-pollen palynomorphs -NPPs), diatoms, peat stratigraphy, geomorphology.	Borromei et al., (2010)
GLACIAR CHATO		Geomorphology	San Martín et al. (2021b)
HARBERTON PEAT BOG	TH	Palynology, plant macrofossils, diatoms.	Heusser, (1989) Savoretti et al. (2017) Savoretti, (2018)
CAMBACERES BAY	BCa	Geomorphology	Zangrandi et al. (2016)
VARELA RIVER	RV	Palynology, palynofacies, geomorphology, sedimentology.	Grill et al. (2002)
LANUSHUAIA MARSH	AL	Palynology, palynofacies.	Candel et al., (2011)
MOAT PEAT BOG	TM	Geomorphology, palynology, plant macrofossils, geomorphology.	Borromei et al., (2014) Savoretti, (2018)
ISLA DE LOS ESTADOS (IDE)			
BAHÍA FRANKLIN PEAT BOG	IDE-1	Palynology, geomorphology.	Ponce et al., (2011) Björck et al., (2012)
BAHIA FRANKLIN PEAT BOG	IDE-2	Palynology, geomorphology.	Ponce et al., (2017)
LAGO GALVARNE PEAT BOG	LGB	Geochemistry, magnetic susceptibility, geomorphology, XRF, diatoms, TC, TN LOI, tephra analysis.	Unkel et al., (2008) Unkel et al., (2010) Fernández et al. (2012), 2014 Ponce and Fernández, 2013
LAGUNA CASCADA PEAT BOG	TCAS	Geochemistry, geomorphology, XRF, diatoms, TC, TN, LOI, biogenic silica, tephra analysis.	Unkel et al., (2008) Unkel et al., (2010) Fernández et al. (2012), 2013 Ponce and Fernández, 2013

et al., 2000). The glaciers from the ice sheet of the Darwin Cordillera (2000 m a.m.s.l., Fig. 2) flowed towards the north and east of Argentinian IGTDF, along wide and deep valleys that currently form the Magellan strait, Bahía Inútil-San Sebastián bay depression, Fagnano lake, Carbajal-Lasifashaj valleys, and BC (Fig. 1 A). The sedimentary deposits and landforms corresponding to the oldest glaciations are found

mainly further north and are associated with the glacial lobes of Bahía Inútil-Bahía-San Sebastián and Magellan strait depression (Coronato et al., 2004; Ponce et al., 2020). The deposits and landforms corresponding to the Last Glacial Maximum (LGM, 24,000 cal yrs. BP, Rabassa, 2008) are the most abundant and best preserved due to the great extension the glaciers reached, when 50% of the Argentinian sector of IGTDF surface (approximately 22,500 km², Fig. 2) was covered with ice (Ponce et al., 2020).

The latitude and insularity favor the development of cold oceanic climates, humid in the south and sub-humid in the north (Coronato et al., 2008), with a mean annual temperature between 5 °C and 6 °C, a S–N decreasing precipitation gradient direction (600–300 mm annually) and a W–E increasing gradient direction (600–2000 mm annually). The distribution of precipitation is strongly influenced by the arrangement of orographic barriers given the movement of cold and humid air masses from the W and S. The SWW, originated in the South Pacific high-pressure system, blow from the NW, W, and SW with different frequency and intensity according to the variability in the position of the system and the influence of the local relief on the air movement, temperature, and humidity. The Polar Front low-pressure system receives these winds and those from the Antarctic high-pressure system, which brings cold air masses from the SW, S, SE and is loaded with moisture when crossing the sub-Antarctic Sea, generating orographic precipitations. These winds are the most constant and intense in the Southern Hemisphere as a consequence of the latitudinal migration of the low atmospheric pressure system between 50 and 70°S and the Southern Ocean dynamic, which connects the ocean basins of the Southern Hemisphere. Therefore, the SWW are one of the most important determinants of the southern climate with implications for the global climate.

In the northern steppe of the Argentinian IGTDF, the wind acts as a desiccation factor and a powerful geomorphological agent. Its frequency is counteracted by the advection of air masses from the Atlantic Ocean, leading to fogs and precipitations with a decreasing E–W gradient. The mean annual temperature of the steppe is 5.5 °C (Tuhkanen, 1992), oscillating between 10.2 °C (January) and 1.2 °C (July) (warmest and coldest months respectively, in the period 2011–2021). The annual mean precipitation oscillates between 190 and 330 mm yr⁻¹. The monthly mean value for the driest month (October) is 8.4 mm.

The central area of the Argentinian sector of IGTDF, the ecotone, shows the highest annual thermal amplitude due to a marked continentality (Tuhkanen, 1992). The average temperatures range between 11 °C in the warmest month (January) and –1 °C in the coldest month (July). Rainfall varies between 350 and 500 mm yr⁻¹.

In the southern zone, rainfall and snowfall feed water and glacial systems that trigger mass removal processes. Ushuaia city shows an average annual temperature of 5 °C, with 9.2 °C for the warmest month (February) and 1 °C for the coldest month (July), while the average rainfall is 550 mm yr⁻¹ (Tuhkanen, 1992). The increasing precipitation gradient from the eastern mouth of the BC towards IDE (Fig. 3) and the absence of orographic barriers to the south of IDE cause rainfall records above 1000 mm yr⁻¹ (Tuhkanen, 1992).

The mountainous wooded area in the south is characterized by the presence of cirque glaciers, relicts of the old alpine glaciers forming the glaciated network that contributed ice and detrital load to the glacier flowing through the BC during the LGM. The glacial coverage in the Argentinean sector of the Fuegian Andes is restricted by the orographic chain in south-central IGTDF, and no glaciers are present in Mitre peninsula (Fig. 1 A) or IDE. A total of 90 small glaciers less than 1 km² have been identified. These are located between 880 and 1380 m a.m.s.l. (San Martín et al., 2021a) while the equilibrium line is located between 1050 and 1150 m a.m.s.l., about 100 m above the isotherm of 0 °C (Iturraspe, 2011). These glaciers are retreating and may become extinct in the coming decades if current climatic conditions persist (San Martín et al., 2021a).

The distribution of plant communities is associated with climatic and

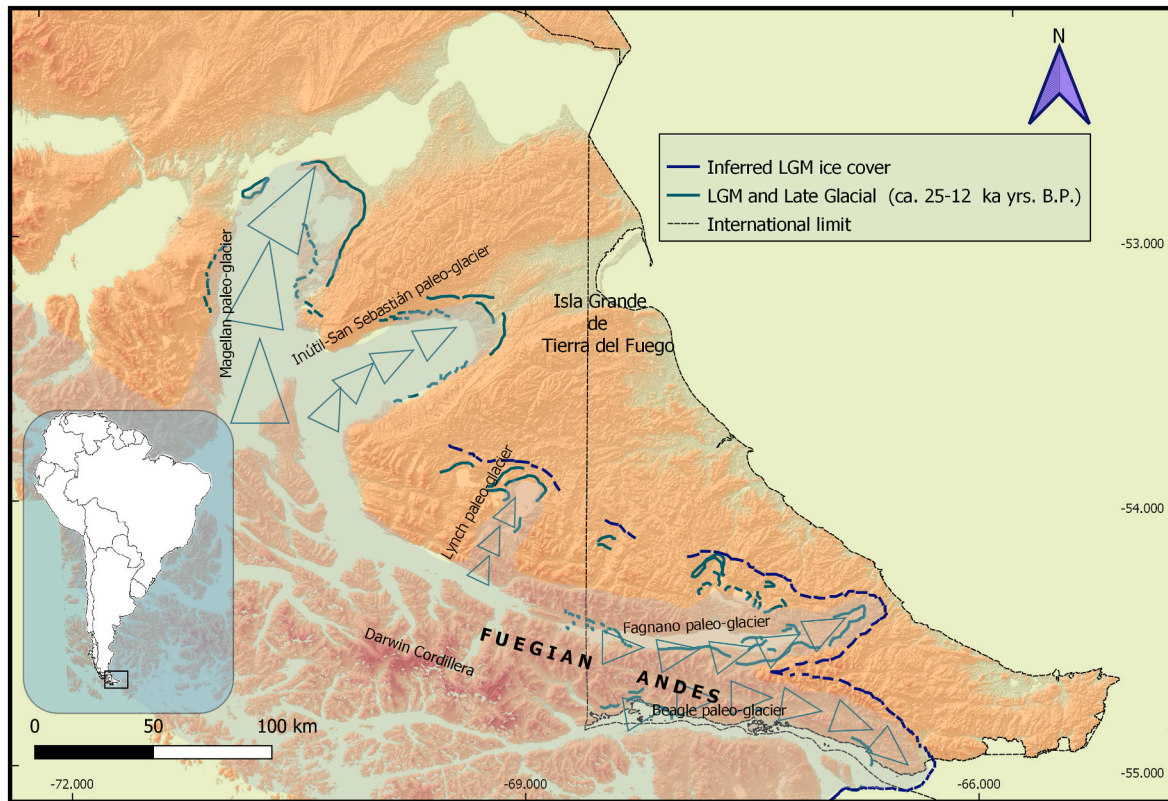


Fig. 2. Ice extent, glacial lobes and glacial limits during the Last Glacial Maximum (LGM) in Tierra del Fuego. (Modified from Coronato et al., 2004 using SRTM-90 m provided by IGN-Argentina).

topographic gradients (Figs. 3 and 4). In the Magellanic moorland, *Donatia fascicularis* and *Astelia pumila* carpet mires cover glaciofluvial plains and lowlands in the eastern sector of the Argentinian IGTDF and IDE, exposed to strong winds, with rainfall >1000 mm yr⁻¹ (Tuhkanen, 1992). The Andi-alpine vegetation, between the altitudinal limit of *Nothofagus* and the snow line, displays shrub species, cushion plants, and herbaceous communities (Moore, 1983). The Evergreen Forest, dominated by *Nothofagus betuloides* accompanied by *Drimys winteri*, *Maytenus magellanica*, and abundant ferns and bryophytes, grows where rainfall exceeds 700 mm yr⁻¹. In some sectors, *Nothofagus betuloides* forests mix with *N. pumilio*, giving rise to a pattern termed mixed forest formation. The Deciduous Forest is characterized by the association of *N. pumilio* and *N. antarctica*. Both species grow to an average altitude of 550–600 m a.m.s.l. and are dominant with annual precipitation above 450 mm (Moore, 1983; Tuhkanen, 1992). In the south of the Argentinian sector of IGTDF, ombrotrophic peat bogs of *Sphagnum* extend in the valley bottoms, intermoric and interdrumlin depressions, and kettles in the Deciduous Forest and, to a lesser extent, in the Evergreen Forest. *Sphagnum magellanicum* dominates, together with a rich flora of other mosses, liverworts, lichens, and vascular plants (Roig, 2004). Contact between the steppe and the deciduous forest occurs through a transitional zone, the Fuegian ecotone. In the steppe, acidophilic, mesotrophic, and neutrophilic vegetation occurs according to the edaphic, topographic, and lithological features (Collantes et al., 1999). Diverse communities are identified along a floristic gradient, ranging from *Chiliotrichum diffusum* scrub and *Empetrum rubrum* dwarf shrub heaths to *Festuca gracillima* tussock grasslands with short grasses (*Poa*, *Trisetum*) and forbs as soil acidity decreases. The minerotrophic peat bogs are in poorly drained sectors between Fagnano lake (LF) and Grande river (Iturraspe, 2010; Loisel and Yu, 2013) and in the western sector of IDE, and are formed by high-density herbaceous vegetation composed of sedges, rushes, grasses, and Bryales (Roig, 2004).

4. Environmental changes recorded in Tierra del Fuego and Isla de los Estados

4.1. Environmental evolution during the Late Glacial-Holocene transition

The formation of peat bogs and the re-colonization of vegetation after the LGM ice retreat in the south and center of Argentinian IGTDF implied significant changes in the biomes. The basal datings of the peat bogs originated in depressions occupied by shallow lakes, lagoons, and proglacial streams, locate and date the onset of the glacier retreat. In the BC, the basal dating of the Harberton peat bog (TH, Fig. 1 A) indicates that the peat bogs formation process started around 19,400 cal yrs. BP (Savoretti, 2018). In the inner valleys of the Fuegian Andes, the Cañadón del Toro peat bog (TCT, Fig. 1 B) originated ca. 13,500 cal yrs. BP (Borromei et al., 2016). In the LF valley (Fig. 1 A), La Correntina (TLC A) and Terra Australis (TTA) peat bogs, located in the eastern and southern sectors of the lake, respectively (Fig. 1 A), indicate a minimum age range between 15,400 yrs. BP and 14,300 cal yrs. BP, respectively (Musotto et al., 2016, 2017b). The IDE-1 peat bog, in the SW of IDE (Fig. 1 A), has a minimum age of ca. 12,600 cal yrs. BP (Ponce et al., 2011), while the base of the core from Laguna Cascada peat bog (TCAS), located in the center of IDE (Fig. 1 A), was dated at 16,000 cal yrs. BP (Unkel et al., 2008; Fernández et al., 2013).

In the south and center of the Argentinian sector of IGTDF, the pollen and plant macrofossil records of TH and other peat bogs show, in general, that the association of herbaceous (Poaceae, *Acaena*, *Caltha*, *Gunnera*, Caryophyllaceae, among others) and shrubby vegetation (Asteraceae subf. Asteroideae, *Empetrum rubrum*) with little participation of *Nothofagus dombeyi*-type arboreal vegetation was the first covering of the ice-free lands and the areas dominated by shallow lakes affected by melt water (Heusser, 2003; Markgraf and Huber, 2010; Savoretti et al., 2017). A modern analog of this type of environment is the Fuegian steppe.

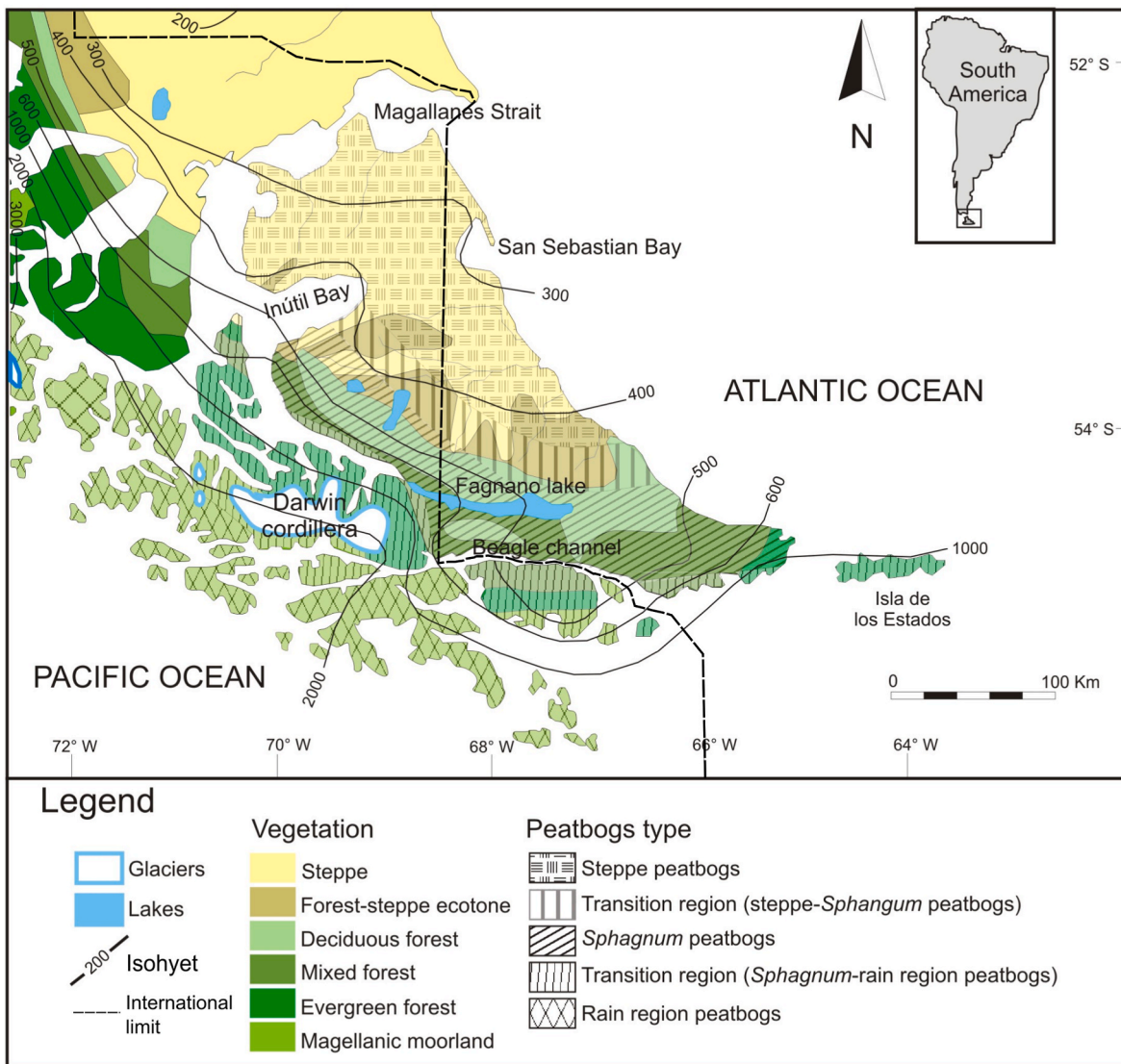


Fig. 3. Forest and peat bogs or mires and precipitation values distribution in Isla Grande de Tierra del Fuego (modified from Musotto et al., 2016).

The Late Glacial-Holocene transition was characterized by the *Nothofagus* expansion, from multiple ice-free refuges (Prémoli et al., 2010) located within the current extension of the forest, while the herbaceous-shrub communities remained. The local presence of *Nothofagus* is inferred from the persistent record of the hemiparasitic plant *Misodendrum*. Besides, the record of coprophilous fungal spores like *Sordaria*-type and *Sporormiella*-type suggests the presence of herbivorous grazers (Musotto et al., 2017a, 2017b). Arbuscular mycorrhizal *Glomus* sp. registered in TLC and TTA is probably related to the development of grassy vegetation associated with communities of the forest-steppe ecotone (Fig. 5). Likewise, the record of pyrophilic-carbonicolous spores of *Gelasinospora* with abundant charred plant remains in these peat bogs suggests the occurrence of fires. According to the evidence of plant macrofossils in TH, the dominance of the bryophyte *Scorpidium revolvens* indicates the development of a minerotrophic or runoff-fed peat bog with detrital input, up to ca. 8700 cal yrs. BP (Savoretti, 2018), consistent with other pollen records of peat bogs in the region showing the predominance of the Cyperaceae (sedges) (Borromei et al., 2016; Musotto et al., 2016, 2017b), supporting the minerotrophic conditions of these environments. The record of dematiaceous spores of *Arthrinium pucciniioides* in TTA (Fig. 1 A) is probably associated with the development of sedges around the peat bog (Musotto et al., 2017b).

The diatom associations identified in TCAS, IDE (Fig. 1 A) and the co-

dominance of *Aulacoseira* spp., *Brevicula arenii* (Fig. 5) and *Stauroforma exiguiformis* allow to infer acidic lake conditions between 12,800–11,100 cal yrs. BP. On the other hand, the presence of *Pinnularia interrupta*, *Stephanodiscus* cf. *rotula*, *Frustulia rhomboidea* and *Eunotia* sp. associated with peat bogs or swampy surfaces (Krammer and Lange-Bertalot, 1986) suggests that non-windy conditions prevailed in this period, favoring aquatic productivity and the development of terrestrial vegetation, which provided the substrate for the development of these species (Fernández et al., 2013). Likewise, the sedimentological analysis and the geochemical record also suggest an increase in the aquatic productivity and gradually warmer temperatures, without glacial influence (Unkel et al., 2008), in comparison with earlier periods.

During the LGM, the steppe was a cold desert with polygonal soils and ice-wedge formation (Pérez Alberti et al., 2008) while the glacial fronts located approximately 100 km to the W, SW, and S of the steppe limits (Fig. 2). Postglacial climatic improvement favored the development of flat-bottomed deflation basins or pans, where seasonal brackish shallow lakes were formed. This is the case of the current shallow lakes Arturo (LA) and Carmen (LC) (Figs. 1 and 3 E), located 73 and 27 m a.m.s.l., respectively, in paleo-drains currently blocked by lake bottom deposits (Villarreal and Coronato, 2017). Perched dunes were formed on their steep coasts, with levels subject to pedogenesis (Coronato et al., 2021).

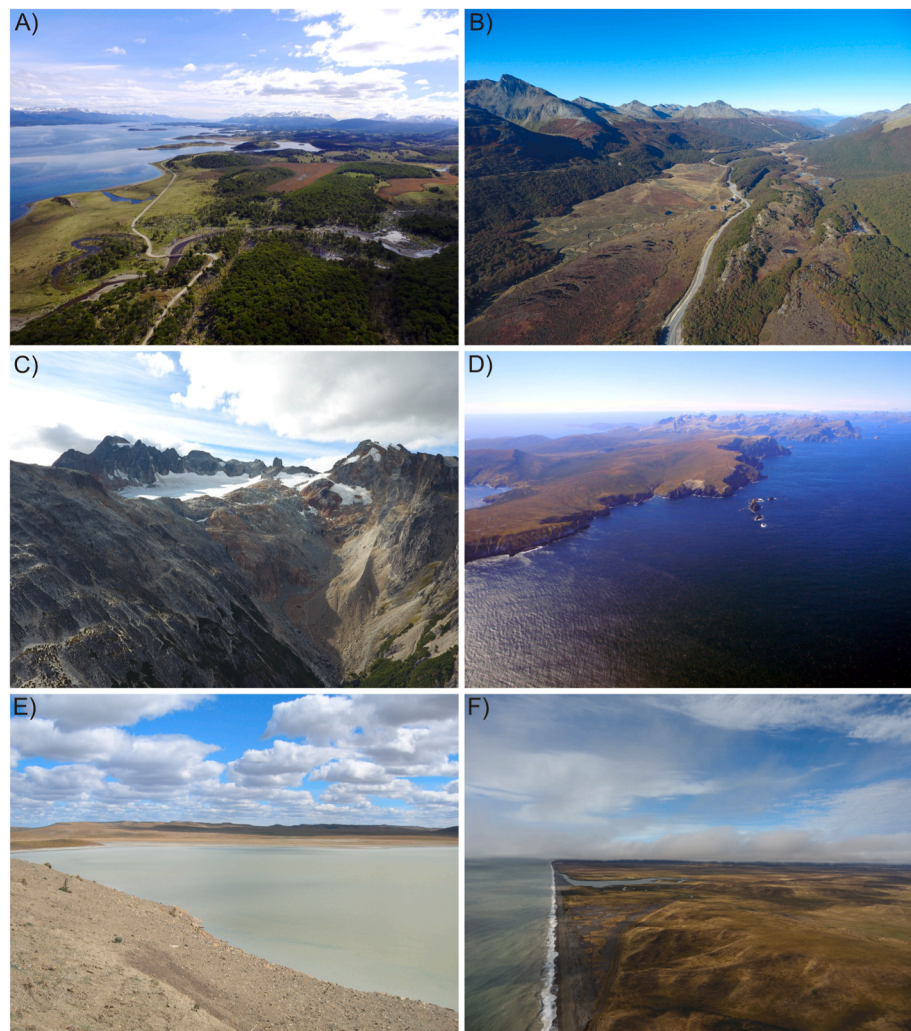


Fig. 4. Landforms and vegetation communities in Isla Grande de Tierra del Fuego. A) North coast of the Beagle channel (to the W) at Harberton range, coastal features and peat bogs developed among drumlins can be observed. B) Inner valleys of the Fuegian Andes covered by peat bogs; *Nothofagus* sp. forest covers the slopes up to 600 m a.m.s.l., approximately. C) Cirque glacier fastly receding in a south-facing slope of one of the Fuegian Andes range; fresh erosive and depositional features can be seen. D) Aerial view of the southern cliff coast of IDE. E) Arturo Lake view in the semiarid northern steppe. F) Linear coastal features along the Atlantic Ocean and the steppe plains.

On the coasts of LA, five levels of lake terraces with a maximum height of 11 m above the current basin floor are observed (Fig. 6). Although the age of these terraces has not been determined yet, their topographic position, geomorphological characteristics, and type of sediment allow us to infer that the shallow-lake occupied an area of 6.6 km², notably greater than the current 1.9 km². A progressive variation in the size of the lake according to the relative unevenness of the terraces with respect to the current bottom lake floor is observed (Table 2).

The multiproxy analysis of the LA core (Table 1) shows the lake persistence during the Late Pleistocene-Holocene transition. The presence of epiphytic diatoms such as *Cocconeis placenta* (Fig. 7) and *Epi-themia adnata* and the co-dominance of taxa that inhabit fresh to brackish waters indicate that, from the Late Glacial to the Middle Holocene, the lake was shallow but permanent, with fresh to brackish waters (Fernández et al., 2020), probably occupying lake levels I to III (Table 2). During the same interval, three paleosol levels (Ps1, Ps2, Ps3) were formed in the perched dune on the cliff of the southern coast of the lake (Coronato et al., 2011, 2021, Fig. 8). The oldest paleosol (Ps1) was dated to 12,830 cal yrs. BP, while Ps2, located 0.90 m above, was dated to 11,290 cal yrs. BP and Ps3, located 1.60 m from Ps1, was dated to 8380 cal yrs. BP (Table 3). Ps2 shows magnetic parameters that, which confirms a high relative humidity during soil formation interval (Orgeira et al., 2012).

Las Vueltas shallow lake (LLV), located in the coastal zone (8 m a.m.s.l., Fig. 1 A), preserves the morphology of a drainage network developed during the Late Pleistocene on sandy-siltstones (Montes et al.,

2020). The multiproxy analysis (Table 1) shows that, between 19,000 and 11,600 cal yrs. BP, the bottom lake sediments were subject to sub-aerial exposure and oxidation, suggesting low water level, desiccation, and isolation from the littoral environment, since the coastline was located on the current continental shelf (Candel et al., 2020). Based on the Sr/Ba ratio and diatom assemblages, an ephemeral fresh-brackish water body with frequent fluctuations in the water level could have occurred under predominantly arid conditions. The record of *Zygnema* zygospores during the Early Holocene indicates the presence of fresh-water and shallow, less than 50 cm depth environments, well-oxygenated, mesotrophic to eutrophic, and subject to seasonal desiccation and increased water temperature. High Rb/Zr values confirm the poor circulation of water in these shallow environments and the deposition of fine-grained sediments, associated with shrub/herbaceous steppe vegetation, mainly composed of Asteraceae subf. Asteroidae, indicating low effective humidity conditions and probably temperate temperatures (Candel et al., 2020).

4.2. Transgressive-regressive marine event during the middle to Late Holocene

The Holocene marine transgression in the Argentinian sector of IGTDF is geomorphologically represented by paleocliffs, beach ridges, barriers, barrier spits, estuarine environments, and marine terraces (Fig. 9). Mid-Holocene raised beaches along the coast of the BC reached maximum elevations of ca. 10 m above storm berms (Gordillo et al.,

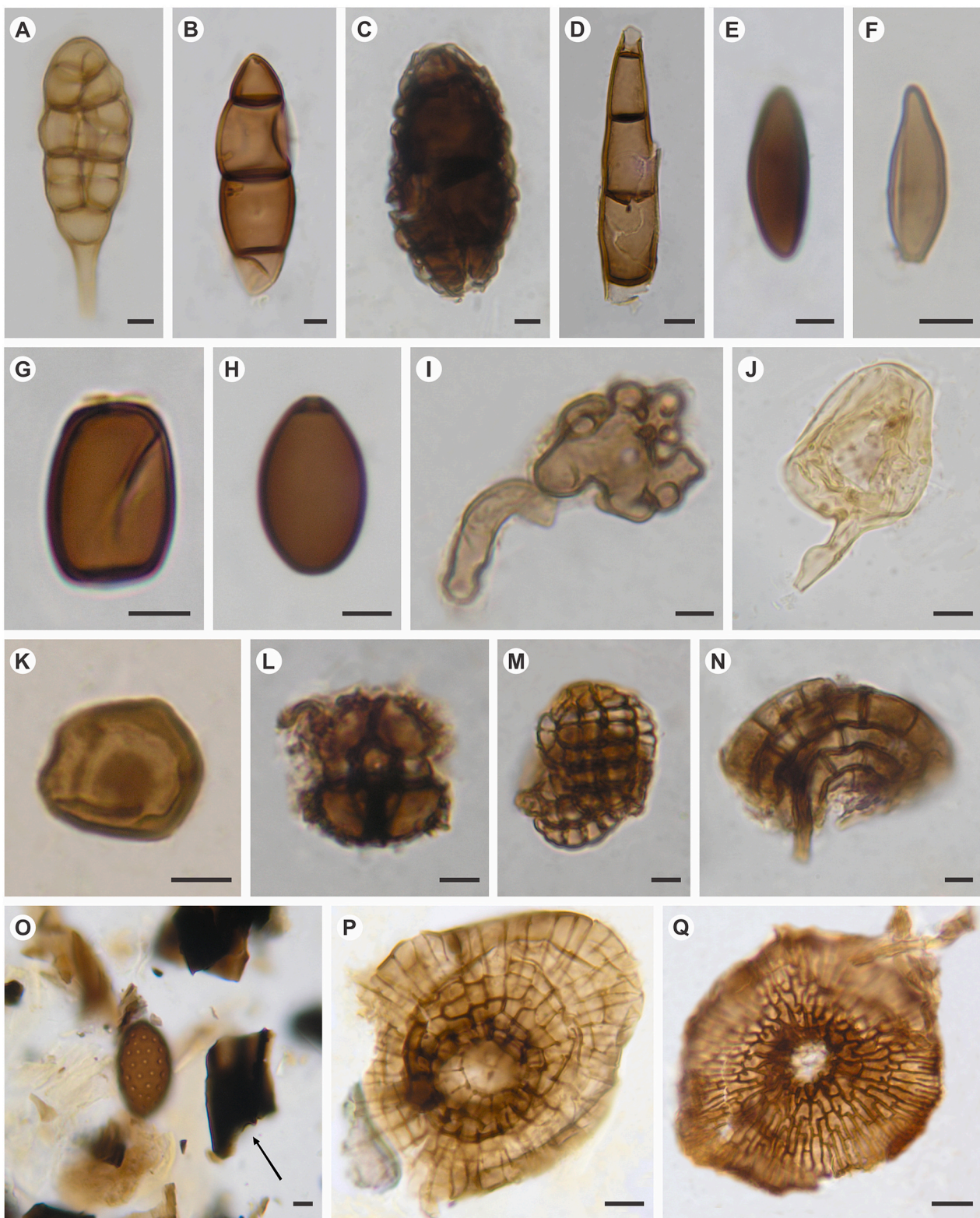


Fig. 5. Main fungal microfossils identified at the La Correntina and Terra Australis peat bogs (modified from [Musotto et al., 2018](#)). Scale bar is 5 µm except in photos D, J, P and Q where the scale bar is 10 µm. Sample number followed by England Finder coordinates. A) *Alternaria* sp., TLC3547-S27. B) Type 810 cf. *Byssothecium alpestre* (fide [Mauquoy et al., 2004](#)) TTA3795-Y27/1. C) *Byssothecium circinans*, TTA4079-Y37. D) cf. *Sporidesmium* sp., TLC3371-M29/2. E) cf. Xylariaceae/Sordariaceae/Coniochaetaceae (fide [Gelorini et al., 2011](#)), TLC3547-J44. F) *Anthostomella* cf. *fuegiana*, TLC3524-Y27/1. G) Separate ascospore-cell of Sporormiella-type, TLC3238-X42. H) Sordaria-type, TLC3522-Y46/1. I) *Gaeumannomyces* sp. hyphopodium, TTA3738-Y41. J) *Glomus* sp., TLC3521-Z33. K) *Arthrinium puccinoides*, TTA4000-U38/4. L) *Spegazzinia tessartha*, TTA3698-B44/4. M) cf. *Dictyosporium* sp., TTA3700-G12. N) Fragment of helicosporous conidium indet. 1, TTA3826-U45. O) *Gelasinospora* sp., TLC3301-Q29/4, arrow shows an oxidized phytoclast. P) Ascomata indet. 2, TLC3241-F29/2 (fide [Musotto et al., 2013](#)). Q) Entire reproductive body of cf. *Microthyrium fagi*, TTA3804-S38/1.

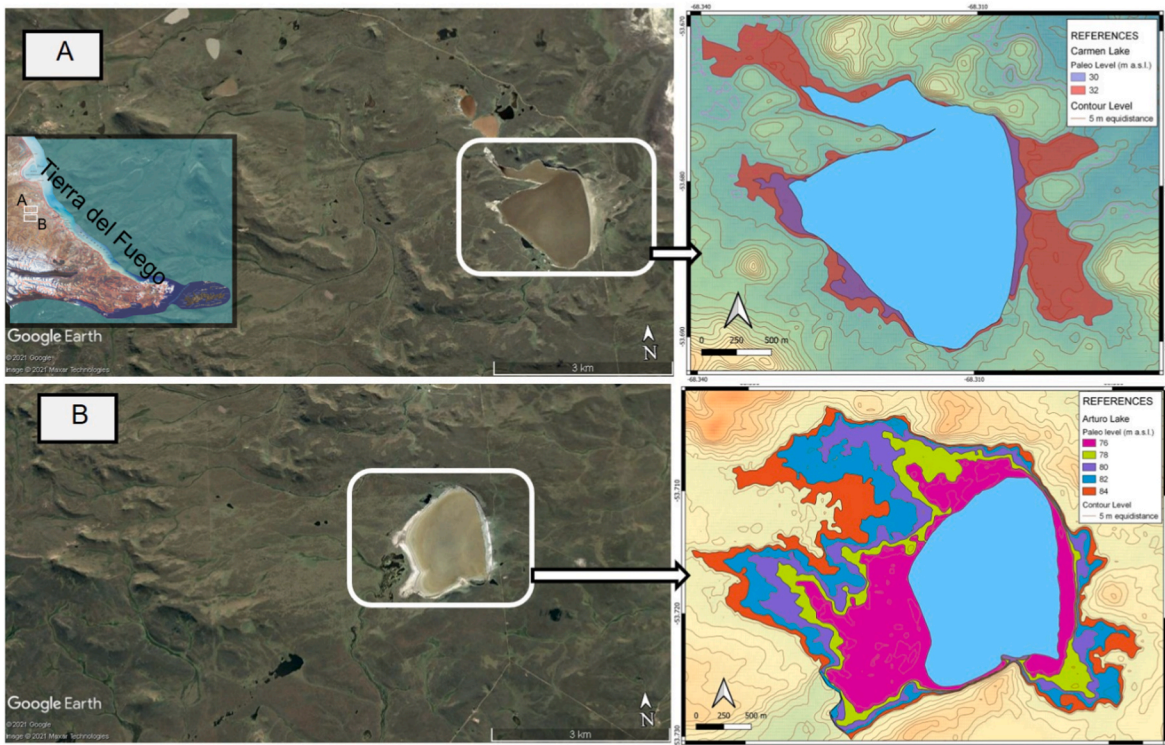


Fig. 6. Paleolevels at Carmen (A) and Arturo (B) lakes interpreted by geomorphological and sedimentological recognition of sedimentary lacustrine terraces. To the left, the entire lake basins relief from Google EarthTM digital model.

Table 2

Topographic position and extent of lacustrine terraces of Carmen and Arturo shallow lakes indicating past lacustrine expansion phases. See Fig. 1 for location.

Carmen shallow lake

	Present	29 m a. m. s.l.	1.9 km ²
Level II	+1 m	30 m a. m. s.l.	2.1 km ²
Level I	+3 m	32 m a. m. s.l.	3 km ²
Arturo shallow lake			
Present		73 m a.m.s.l.	1.9 km ²
Level V	+3 m	76 m a.m.s.l.	3.3 km ²
Level IV	+5 m	78 m a.m.s.l.	4 km ²
Level III	+7 m	80 m a.m.s.l.	4.8 km ²
Level II	+9 m	82 m a.m.s.l.	5.8 km ²
Level I	+11 m	84 m a.m.s.l.	6.6 km ²

1992; Bujalesky, 2007; Björck et al., 2021). However, five levels of raised beaches between 1.5 and 10 m a.s.l. at Playa Larga (Gordillo et al., 1992; Fig. 1 B), the raised beaches and paleociffs ca. 5 m above storm berms in Cambaceres bay (BCa) (Zangrandó et al., 2016, Figs. 1 A and 9 A), and the subsidence in Sloggett bay (BS, Rabassa et al., 2003) reveal the complexity of the tectonic and glacio-isostatic activity along the Beagle Channel. Porter et al. (1984) presents altimetric data and radiocarbon dating from the BC and the Magellan strait (Chile), attributing the differences to isostatic and hydro-isostatic deformation of the crust resulting from changing ice and water loads. Conversely, in a tectonically more stable context, far from the glacial fronts, the mid-Holocene coastal ranges of the Atlantic coast, in the Bueno and Chico rivers area and in San Sebastián bay (Figs. 1 and 8 B, C and D, respectively), are located between 1.5 and 2.7 m above the current storm berm (Montes, 2015; Montes and Martinioni, 2017; Bujalesky et al., 2021).

According to the bathymetry of the Beagle and Murray channels (Fig. 1 A) and a tectonic uplift of 1.3 mm/yr⁻¹ calculated from elevated beaches on the north coast of the BC, it has been suggested that the

trough occupied by the BC was flooded by the sea through the Mackinlay pass, the Murray channel, and the Northwest and Southeast channels (Fig. 1 A), which previously made up watersheds (Bujalesky, 2011) or rocky thresholds. The flood would have occurred quickly immediately after 11,000 cal yrs. BP, when the rising sea level exceeded the current bathymetric thresholds, about 30 m below the current sea level. The paleogeographic evolution at Punta Moat (PM, Fig. 1 A) indicates that the sea would have reached this sector around 10,000 cal yrs. BP (Borromei et al., 2014).

Evidence from Roca lake (LRo) and Lapataia bay (BL) (Fig. 1 B), on the north coast of the Beagle Channel, indicate that the marine environment was established around 8300 cal yrs. BP (Rabassa et al., 1986, 2009a; Gordillo et al., 1993, 2013; Borromei and Quattroccchio, 2007; Candel et al., 2018). These records agree with the chronology proposed for the south coast of the channel around 8640 cal yrs. BP (McCulloch et al., 2019) and 8500 cal yrs. BP (Björck et al., 2021).

The Holocene marine deposits on the north coast of the Beagle Channel are composed of coarse sands alternating with pebble layers. Due to the geomorphological structure of the channel, the deposition of clay sediments may have been confined to small sectors (Gordillo et al., 1993; Rabassa et al., 2009a), except for the Río Ovando (RO)-Cormoranes Archipelago area (ArC) (Fig. 1 B), where the lake-river connection to the sea may have allowed seawater to enter at least 4 km inland from BL (Gordillo et al., 1993).

The paleoenvironmental reconstruction of the transgressive-regressive event at the BC is limited to different time windows because Middle-Late Holocene sedimentary deposits are scattered. Between 8300 and 6200 cal yrs. BP, aquatic palynomorph assemblages identified in BL, Aserradero-Lapataia 2 (As) and Río Varela (RV) localities (Fig. 10 B) are characterized by a low dinocyst diversity, mainly *Brigantedinium* spp. and *Selenopemphix* sp., and other marine taxa, with high participation of freshwater algae (*Spirogyra* and *Zygnea* sp., Fig. 7), indicating an environment with low and variable salinity, temperate-cold water temperature, and abundant nutrients due to freshwater input by surface runoff (Grill et al., 2002; Borromei and

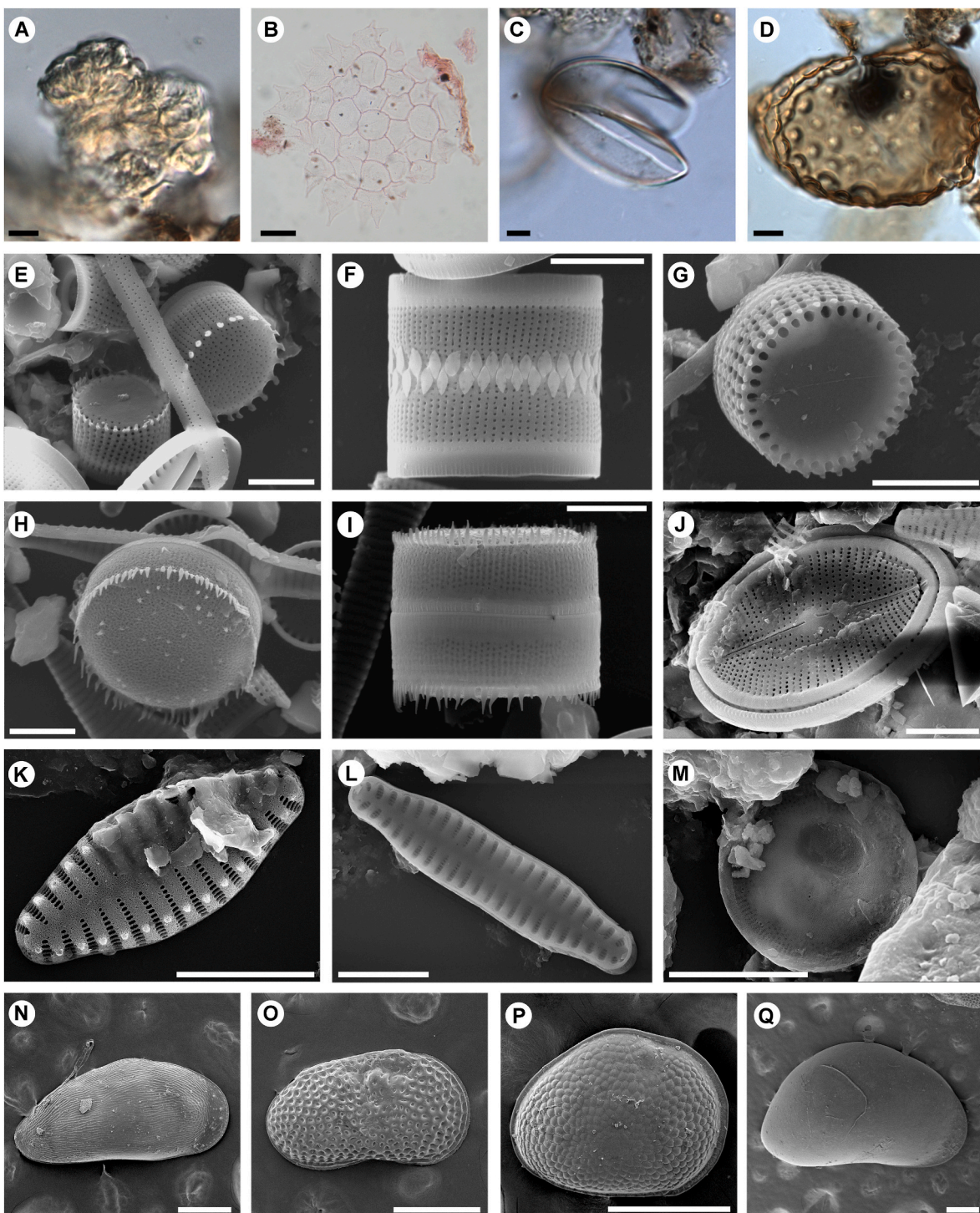


Fig. 7. A–D: Photomicrographs of freshwater to brackish water algae identified in fossil marine sediments from the Beagle Channel (modified from Candel et al., 2018) and from Carmen Lake in the Fuegian steppe. Scale bar: 10 µm. Sample number followed by England Finder coordinates. A) *Botryococcus* sp., AS40-D31/4; B) *Pediastrum* sp., LC4276a-V23; C) *Spirogyra* sp., AS1-Z46/2; D) *Zygnea* sp., AS19-H15/3. E–M: SEM micrographs of diatoms from Isla de los Estados (modified from Fernández et al., 2012, 2013) and Arturo Lake (modified from Fernández et al., 2020). Scale bar: 5 µm. E) *Aulacoseira distans*, valve face and mantle; *Aulacoseira alpigena*, external valve view. F) *A. alpigena*, girdle view. G) *Aulacoseira perglabra*, valve face. H–I) *Brevisira arenii* (H: external valve view; I: girdle view). J) *Cocconeis placentula*, valve view; K) *Staurosira* sp., valve view. L) *Staurosira binodis*, internal view. M) *Thalassiosira patagonica*, internal view. N–O: SEM micrographs of ostracod species identified in Carmen Lake (modified from Borromei et al., 2018). Scale bar: 250 µm. RV: right valve. N) *Eucypris virgata*, adult female, RV: in external lateral view. O) *Limnocythere rionegroensis* Morph II, adult female, RV in external lateral view. P) *Newhamia patagonica*, adult female, RV in external lateral view. Q) *Riocyparis whatleyi*, adult female, RV in external lateral view.

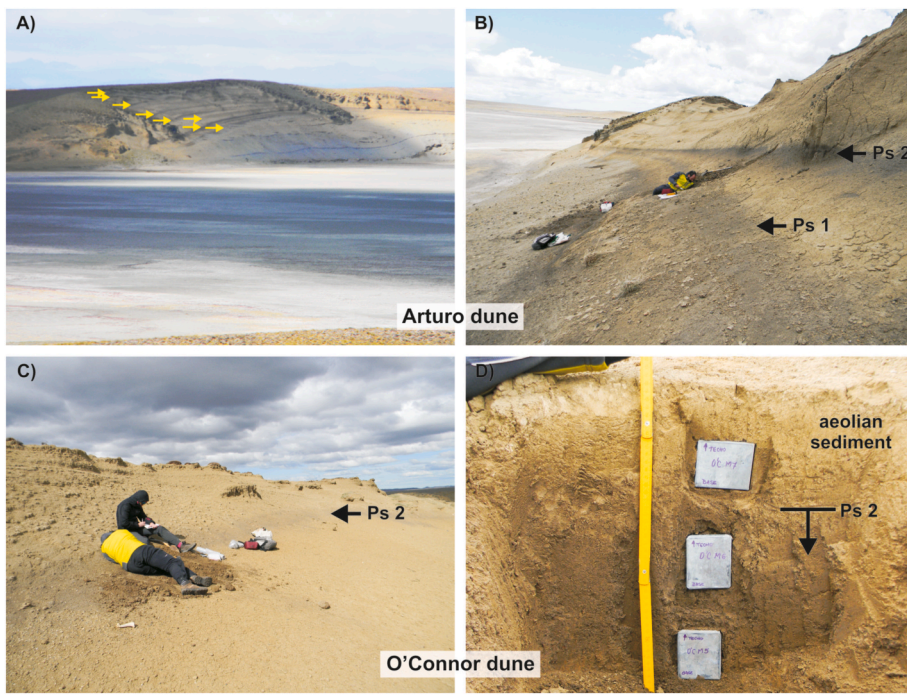


Fig. 8. Paleosols in perched dunes. A) View to the south of Arturo Lake in a seasonal desiccation stage and the Arturo perched dune. Eight dark and continuous sedimentary levels (yellow arrows) corresponding to the Holocene paleosols sequence are observed. B) Sampling paleosols 1 and 2 (Ps1, Ps2) at the base of the dune. C) Upper levels of O'Connor perched dune and paleosol 2 (Ps2), Late Holocene in age. Ages varied from ca. 12,830 cal yrs. BP (Ps1 Arturo dune) to ca. 1800 cal yrs. BP (Ps2 O'Connor dune) showing that periods of humidity and less wind action allowed edaphization in aeolian deposits of the Fuegian steppe all along the Holocene. D) Ps2 detail and sampling with Kubiena-type boxes. See Table 3 for dates of each paleosols.

Table 3

Radiocarbon and calibrated ages for Arturo dune paleosols (CALIB REV8.2 after Stuiver and Reimer, 1993. Calibration data set: shcal20.14c, after Hogg et al., 2020).

Laboratory code	Uncalibrated age (^{14}C yrs. B.P.)	Calibrated age (yrs. B.P.; median probability)	1 σ range	2 σ range
Ps 8	AA95362	960± 27	842	864–903
Ps 7	AA95635	2699± 40	2778	2742–2787
Ps 6	LP-3368	4430± 100	5023	4854–5054
Ps 5	AA95367	4443± 43	4998	4870–5047
Ps 4	AA95368	5787± 46	6550	6491–6629
Ps 3	AA95369	7614± 49	8384	8345–8419
Ps 2	AA95370	9907± 59	11,268	11,202–11,318
Ps 1	AA95371	10,945± 61	12,831	12,755–12,849

Quattrocchio, 2007; Candel et al., 2018). According to the palynological records of Albufera Lanushuaia (AL), Arroyo Baliza (AB), and RO (Fig. 1 B), after 6000 cal yrs. BP, the entry of seawater into the channel was accompanied by an increase in the diversity of dinocyst species, acritarchs, foraminifera, and copepod eggs (Candel et al., 2009, 2011, 2017, Fig. 9). This period was characterized by the development of estuarine environments rich in nutrients, contributed by surface runoff, and low to moderate salinities, where *Brigantedinium* spp. was the dominant taxon.

Between 7500 and 4400 cal yrs. BP benthic foraminifera and ostracod at LRo, Golondrina bay (BG), Los Castores creek (ALC), and ArC and RO sections (Fig. 1 B, Table 1) are represented by *Elphidium alvarezianum*, *E. macellum*, *Cibicides dispers*, *C. aknerianus*, *Buccella peruviana*, as well as *Procythereis torquata* and *Austraurilla theeli*, respectively (Gordillo et al., 2013). The species are typical of littoral environment with epifaunal species of foraminifera and ornate ostracods that indicate medium energy, oxygenated sandy substrates (Whatley and Cusinsky, 2002; Bernasconi et al., 2018).

Towards the Late Holocene, an increase in the number and diversity of microplankton assemblages points to an increase in salinity in the BC waters and the gradual establishment of the present-day marine conditions (Candel et al., 2017). The palynological assemblage of AB (Fig. 1 B) is similar to that documented in the modern sediments of the Beagle Channel, suggesting that the current climatic and environmental conditions were established at ca. 3500 cal yrs. BP. Benthic foraminifera identified in AB suggests a gradual change from cold and oxygenated water conditions to shallow, lower-energy environments, as shown by a

decrease in the genus *Buccella* and an increase in *Elphidium* species (Bernasconi et al., 2021, in press). Dinoflagellate cyst assemblages recorded in modern marine sediments reflect estuarine conditions affected by freshwater discharge, with abnormally low salinity for a marine environment (Candel, 2010).

The analysis of the marine malacofauna of the Beagle Channel made it possible to identify a group of pioneer species, which appeared in the Early Holocene, ca. 8500–8300 cal yrs. BP, composed of three epifaunal species (*Mytilus chilensis*, *Aulacomya atra*, and *Pachysiphonaria lessoni*) and two infaunal species (*Mulinia edulis* and *Yoldia woodwarddi*). This group diversified between 7500 and 6000 cal yrs. BP and towards the beginning of the Late Holocene, ca. 4500–3900 cal yrs. BP (Gordillo et al., 2013). Within this ca. 4000-yr interval, greater seasonal amplitude and higher summer temperature have been identified, in comparison with other earlier and later periods, ca. 5200 and ca. 400 yrs, respectively (Gordillo et al., 2015). Given the heterogeneity of habitats in the BC bottoms, benthic species formed different local paleocommunities depending on the depth, sediments, and types of bottoms, with the presence of infaunal, epifaunal, and mixed communities (Gordillo, 1999; Gordillo et al., 2008, 2013).

The first evidence of the Holocene marine transgression in IDE (Fig. 1 A) was identified in the record of Lago Galvarne peat bog (TLGB, Fig. 1 A), between 8600 and 8000 cal yrs. BP, through the presence of marine dinocysts *Brigantedinium* spp., *B. simplex*, *Islandinium minutum* and *Votadinium calvum*, accompanied by foraminiferal linings and marine-brackish algae such as *Tasmanites* sp. This assemblage suggests a

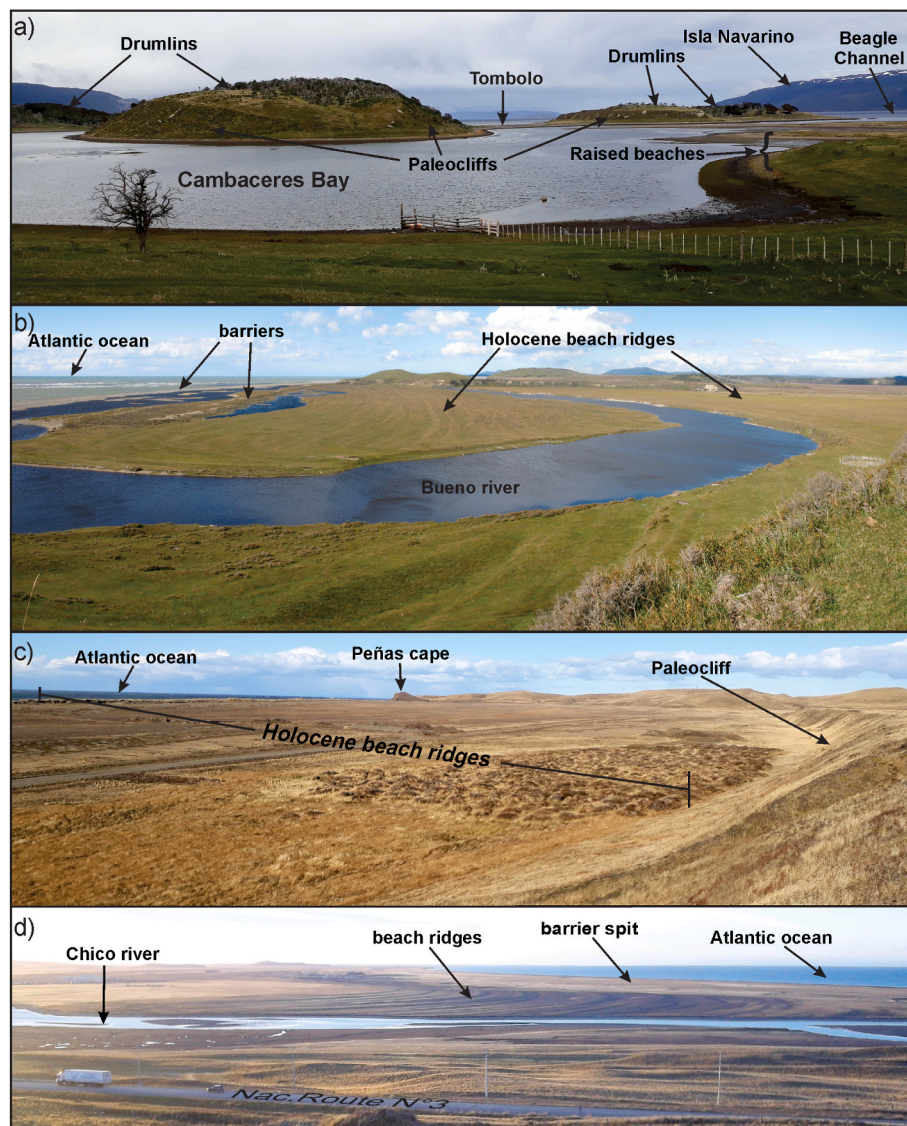


Fig. 9. Holocene littoral landforms A) Cambaceres bay (BCa) at the Beagle Channel north coast. B) Bueno river, in Mitre Peninsula. C) Chico river and D) Bahía San Sebastián in the Atlantic Ocean coastline. The paleociffs were developed during the maximum extent of the marine transgression (8500-6000 cal yrs. BP) and the depositional landforms have been filling the embayments since that time.

marine-marginal environment, with low to moderate salinity and high concentrations of nutrients in the surface waters, probably due to the freshwater input by surface runoff. Brackish-marine diatoms between 8000 and 7400 cal yrs. BP, suggest a strong marine influence. Marine regression is evident after 7400 cal yrs. BP, when a lagoon with limited marine connection, strongly influenced by fluvial discharge, appears to have developed, as indicated by assemblages dominated by fresh to brackish water forms, including *Zygnemataceae* and *Botryococcus* sp. (Fernández et al., 2014).

On the Atlantic coast of IGTDF, the Holocene transgression, the wave-energy, and the strong SWW gave rise to extensive littoral landforms, consisting mainly of gravel and sand, formed by the reworking of Cenozoic sediments and glaciogenic deposits (Bujalesky, 1998; Isla and Bujalesky, 2000). San Sebastián bay (Fig. 1 A) exhibits an extensive coastal plain, partially closed by a gravel spit, the El Páramo peninsula (Bujalesky et al., 2001). After the rise and stabilization of the postglacial sea level, different sedimentary processes took place (Bujalesky, 1997). Estuarine facies were recognized recording the transgressive phase, while littoral ridges and cheniers were deposited during the regressive phase (Bujalesky, 2007). The topographically depressed areas were

filled by the sea, forming bays limited by paleo cliffs and littoral barriers filled with sediments from the Middle Holocene (Bujalesky, 2007). The start of the regressive sequence has not been accurately dated, but radiocarbon dating indicates a minimum age of 5620 cal yrs. BP (Vilas et al., 1999). These processes gave rise to extensive beach ridge plains, causing the retreat of the cliffs and tending to rectify the coastlines at the mouth of Chico, Fuego, Leticia, and Bueno rivers (Bujalesky et al., 2001; Montes and Martinioni, 2017; Montes et al., 2018). In La Misión mire (Fig. 1 A) environments associated with marine transgression were identified (Auer, 1959, 1974) between 8700 and 2700 cal yrs BP, showing diatoms and ostracods typical from brackish-marine environments (Markgraf, 1980, 1993). Unlike the heights described for the BC during the transgressive phase, the sea level reached between 1.55 and 2.69 m above the current level (Bujalesky et al., 2021). As the sea level rose between 8500 and 8100 cal yrs. BP, LLV became a lagoon connected to the sea, where marine dinocysts such as *Spiniferites* sp. and *Oculodinium centrocarpum* were recorded and halophyte vegetation was dominant. During the regressive phase, the lagoon gradually lost its connection with the sea and coastal vegetation developed with expansion of grasses (Poaceae) along with halophytes (Chenopodiaceae). After

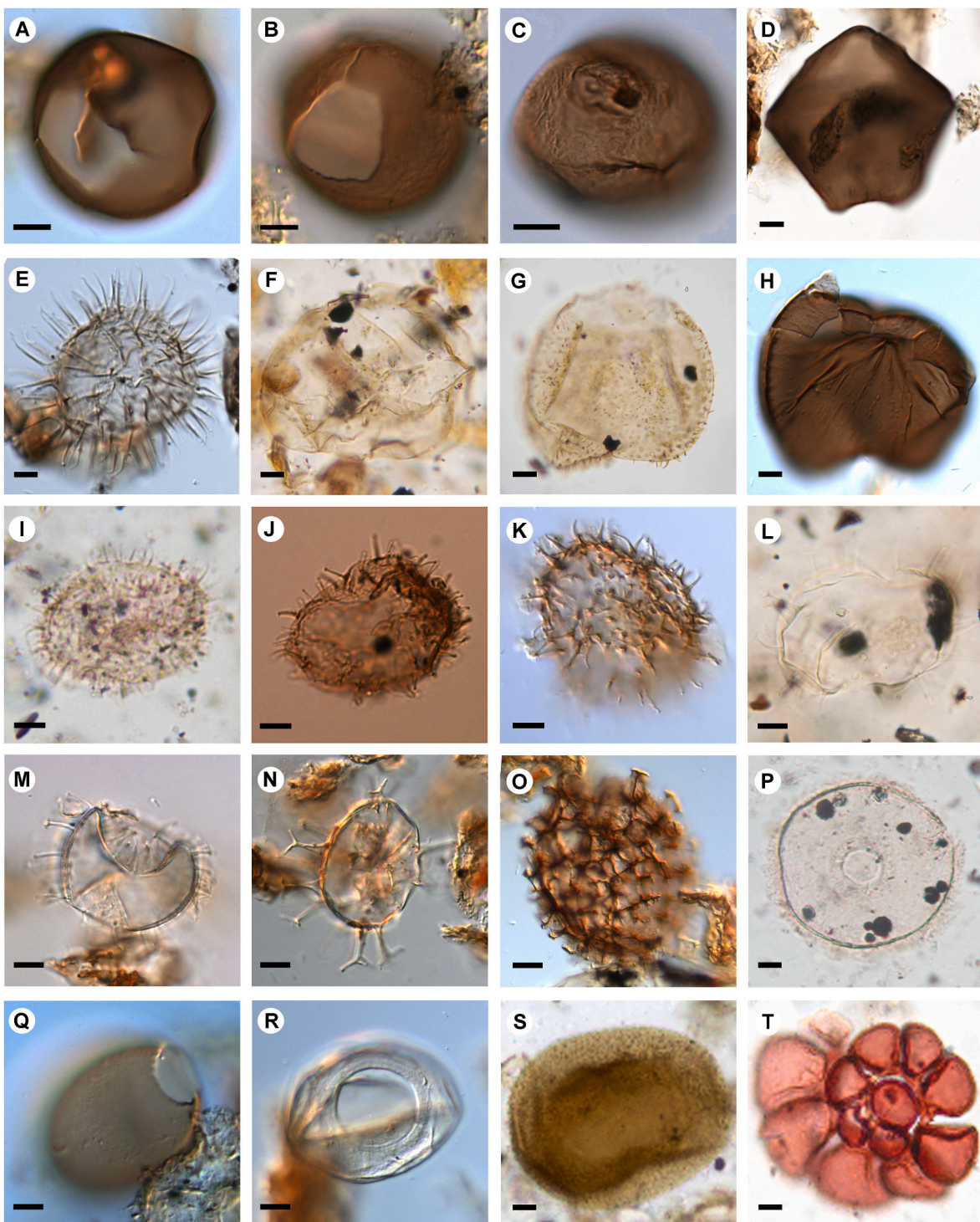


Fig. 10. Main aquatic palynomorphs identified in fossil marine sediments from the Beagle Channel (modified from Candel and Borromei, 2016). Scale bar is 10 μm . Sample number followed by England Finder coordinates. A) *Brigantedinium cariacense*, AB25-B25/2. B) *Brigantedinium simplex*, AB9-A33/2. C) *Dubridinium* sp., AB22-S20/3. D) *Quinquecuspis concreta*, AB5-P35/4. E) *Selenopemphix quanta*, AS49-P45. F) *Selenopemphix nephroides*, BL1631a-C22/2. G) *Votadinium spinosum*, AL2638-Q47/4. H) *Votadinium calvum*, AB21-V25. I) *Islandinium minutum*, RO1968-S14/2. J) *Islandinium cezare*, AB18-U20/1. K) *Echinidinium granulatum*, AB11-W41. L-M) *Operculodinium centrocarpum*, RV1532a-F23/3; AB18-W36. N) *Spiniferites ramosus*, AB1-Q24/4. O) *Polykrikos schwartzii*, AB4-O13. P) *Halodinium* sp., RO1972c-R13. Q) *Palaeostomocystis fritilla*, AB12-J25/2. R) *Palaeostomocystis subtilitheca*, AB10-H11/1. S) Copepod egg, RO1972c-G14/2. T) Foraminiferal lining, RO1972d-G34/4.

7000 cal yrs. BP, the formation of a baymouth barrier and a beach ridge plain blocked the connection of the lagoon, starting the development of gramineous vegetation and the retraction of halophyte plant communities (Candel et al., 2020). Finally, the coastal lagoon was transformed into the current brackish, shallow lake or ‘pan’, with water level

variations controlled by hydro-climatic variables (Montes et al., 2020).

4.3. Wet-dry oscillations during the middle to Late Holocene

The geomorphology of the Fuegian Andes has not yet provided

enough evidence of glacial advances during the Holocene. Menounos et al. (2013) recorded evidence of glacial advances in the cirques of the Fuegian Andes, occurred sometime between 7960 and 7340 cal yrs. BP and 5290–5050 cal yrs. BP. However, they were only tens of meters ahead of the maximum ice position reached during the cooling phase from the fourteenth to the nineteenth century, known as Little Ice Age (LIA).

The pollen record from the south of the Argentinian sector of IGTDF does not show clear evidence of coldest periods associated with neoglacial advances. However, the pollen record from peat bogs in the interior valleys of the Fuegian Andes (Borromei et al., 2016), in center-south of IGTDF (Waldmann et al., 2014; Musotto et al., 2016, 2017b), and in Bahía Franklin (TBF) in IDE (Fig. 1 A) (Ponce et al., 2011) show an increase in the relative frequencies of arboreal pollen from ca. 6700 cal yrs. BP, with the highest pollen concentration values between ca. 5500–3000 cal yrs. BP. From these records, the development of closed-canopy *Nothofagus* forest is interpreted as cold and wetted conditions than in previous periods. Similarly, the fungal assemblages identified in Terra Australis (TTA) and La Correntina (TLC) peat bogs characterized by the Type 810 cf. *Byssothecium alpestre*, *Byssothecium circinans*, *Gaeumannomyces* sp., *Alternaria* sp., and *Anthostomella* cf. *fuegiana* also suggest more humid conditions linked to the development of forest communities (Musotto et al., 2017a, Fig. 5). During this period, in TTA (Fig. 1 A), the record of *Spegazzinia tessartha*, as well as the remains of reproductive bodies of cf. *Microthyrium fagi*, indicates the presence of the Deciduous Forest since both species have been reported in association with *Nothofagus pumilio* (Arambarri and Gamundi, 1984; Godeas and Arambarri, 2007). In the pollen records, the sharp decrease in Cyperaceae (sedges) and the increase in *Sphagnum* (moss) spores reflect an important hydrological shift from ca. 6700 cal yrs. BP in TTA and TCT, and 5300 cal yrs. BP in TLC (Borromei et al., 2016; Musotto et al., 2016, 2017b). The plant macrofossils in TH exhibit a remarkable rise in the concentration of *Sphagnum magellanicum*, suggesting the development of an ombrotrophic peat bog under cold conditions and higher effective humidity. This new hydric situation implied a decrease in the contribution of nutrient-rich surface runoff, replaced with precipitation water. This peat bog experienced rapid growth (0.1 cm yr^{-1}) relative to the growth rate of the previous minerotrophic peat bog stage (0.04 cm yr^{-1}) (Savoretti, 2018). Towards the southeast, the pollen profile of Moat peat bog (TM, Fig. 1 A) indicates that the maximum ombrotrophic development occurred after ca. 5500 cal yrs. BP (Savoretti, 2018). The high frequencies of *Empetrum rubrum* are related to the peat bog itself, since these shrub species colonize the dry *Sphagnum* hummocks, while the low representation of sedges (Cyperaceae) and grasses are associated with their minerotrophic marginal areas or lags (Borromei et al., 2014; Musotto et al., 2016).

The shallow lakes of the Fuegian steppe are characterized by geomorphological and environmental variations, as well as the formation of paleosols in the perched dunes associated with coastal cliffs (Coronato et al., 2012, 2021). During the Middle Holocene, three levels of paleosols (Ps4, Ps5, and Ps6) developed in Arturo perched dune (DA, Fig. 1 A) between 6650 and 5000 cal yrs. BP, with parent material of aeolian origin, and two other levels developed during the Late Holocene, dated to 2780 cal yrs. BP and 840 cal yrs. BP (Ps7 and Ps8, respectively). Likewise, in O'Connor dune, its Ps2, dated to 1800 cal yrs. BP, was recorded (Figs. 1 A, Fig. 8). It is located on the north coast of O'Connor shallow lake on a 17 m cliff formed by siltstones underlying a thin sandy gravel bed (Coronato et al., 2021). The aeolian sediments underlying Ps2 exhibit incipient pedogenesis (dotted brown-dark brown coloration or aggregation of the sediment), but they did not reach the conspicuous formation of a paleosol (Fig. 8 C and D). Around 6000 cal yrs. BP, shortly after the formation of Ps4 in AD, a lowering in the water level of the Arturo shallow lake located at the foot of the dune, would have favored the penetration of light, allowing the development of submerged vegetation, as evidenced by the presence of oogonia of *Chara* spp. towards 3200 cal yrs. BP. The diatom *Surirella tuberosa*, common in semi-terrestrial environments (Frenguelli, 1924a,b), replaced the

planktonic species *Thalassiosira patagonica* (Fig. 7). In addition, the presence of the ostracod *Limnocythere rionegroensis* indicates a lacustrine retraction and enhanced salinity of the waters due to evaporite concentration, which implies that the lake gradually changed to an ephemeral, shallow, saline water body during the Middle-Late Holocene (Fernández et al., 2020). This trend towards the retraction of the water body continued during the Late Holocene, giving rise to the current pan, sensu Villarreal and Coronato (2017).

In Laguna Carmen (LC, Fig. 1 A), the multiproxy analysis of the LCTF-2 core indicates the development of local grassland vegetation (Poaceae) and scattered shrubs (Asteraceae subf. Asteroideae and *Empetrum rubrum*) between ca. 4200–1400 cal yrs. BP. During the last ca. 1400 cal yrs. BP, a greater variability is observed in the plant communities, which fluctuated between grasslands and scrublands. The variations in the relative frequencies of halophytes, algae, and ostracods suggest fluctuations in the water level, which reveals alternating wet and dry intervals throughout the record (Borromei et al., 2018). The wet intervals roughly occurred between 3600–3000, 2700, 2100–1900, and 1600–1400 cal yrs. BP, while dry intervals took place between 4200–3600, 3000–2800, 2600–2100, 1900–1600 and 1400 cal yrs. BP. The wet intervals were characterized by the expansion of grasses (Poaceae), the retreat of halophyte vegetation (Chenopodiaceae), records of hygrophilous taxa such as *Myriophyllum* and *Tetronium magellanicum* and sedges (Cyperaceae), the proliferation of *Pediastrum*, and a sharp decrease in the ostracod *Limnocythere rionegroensis* Morph. II ostracods, together with the predominance of *Riocypris whatleyi* and *Newnhamia patagonica* (Fig. 7). This set of biological indicators suggests a rise in the shallow lake water level with a greater influx of freshwater, nutrient supply, and oligohaline conditions. The analysis of palynofacies indicated for these wet intervals a significant contribution of large, mostly biostructured, well-preserved, translucent phytoclasts, suggesting the proximity to the source of terrigenous material transported by river runoff. The lithology of these wetter intervals consisted mainly of sandy-silty sediments and sand lenses, suggesting an increment in sediment input to the shallow lake by tributary streams during periods of higher rainfall frequency or intensity. On the other hand, the dry intervals show a decrease in grasses (Poaceae), expansion of shrub (Asteraceae subf. Asteroideae) and halophyte (Chenopodiaceae) vegetation, along with predominant *Botryococcus braunii* and *L. rionegroensis* Morph. II, suggesting mesohaline or slightly alkaline conditions, high conductivity, increased evaporation, and probably a low water level of the lake linked to an ephemeral water body resulting from lower rainfall. Although as mentioned above these intervals show a predominance of translucent phytoclasts, also evidences of bacterial-induced degradation was observed on palynomorphs, indicating restricted circulation and suboxic to anoxic conditions. The lithology of these drier intervals corresponded to massive silt-clayey sediments.

The trends reconstructed from the analysis of the LCTF-1 core (Laprida et al., 2021) suggest slightly wetter conditions around 4000 cal yrs. BP, followed by a continuous aridification trend throughout the Late Holocene occasionally interrupted by short-term humid events. A likely climatic threshold at 2200 cal yrs. BP triggers the establishment of semi-arid conditions, with dominant aeolian input over runoff to the lake, as evidenced by the existence of massive structures, the net predominance of *L. rionegroensis* at some levels (>60% and still monospecific assemblages) and reconstructed salinities (obtained by means of a transfer function specifically developed for South Patagonia) in the high oligohaline range (>4000 $\mu\text{s cm}^{-1}$). In general, the wet/dry conditions were characterized by an increase/decrease in the sedimentary grain size, a higher/lower concentration of detrital indicator elements (Fe, Ti), an increase/decrease in the magnetic susceptibility (κ), and relatively low/high values of electrical conductivity.

4.4. Medieval Climate Anomaly

The warm climate event recorded in Europe between the ninth and

eleventh centuries is known as the Medieval Climate Anomaly (MCA) after [Grove and Switsur, \(1994\)](#) and [Hughes and Diaz \(1994\)](#). The interval length was calculated according to dendrological analyses of extratropical trees in the northern hemisphere ([Esper et al., 2002](#)).

In the Argentine sector of IGTDF, little evidence has been reported indicating an increase in temperature coeval with the MCA. [Mauquoy et al. \(2004\)](#) observed desiccation attributed to the MCA in the Andorra valley peat bog (TAV, [Fig. 1A](#)) between 990 and 930 cal yrs. BP. [Waldmann et al. \(2010\)](#) recognized the MCA in a sedimentary core from Lago Fagnano (LF) ([Fig. 1A](#)), based on a lowering iron content interval interpreted as lowering in precipitation coupled with glacier retreat. The analysis of plant macrofossils in TH shows a marked drop in *S. magellanicum* associated with drier and somewhat warmer conditions around 740 cal yrs. BP ([Savoretti, 2018](#)). In the TM, an increase in the diversity of bryophytes and lichens around 1080 cal yrs. BP, possibly also associated with the establishment of more temperate and drier conditions, was inferred ([Savoretti, 2018](#)).

4.5. The Little Ice Age cooling

The Little Ice Age (LIA) comprises a period when glaciers in mountainous areas of the world were generally larger than at present. It was a cold climate event occurring between 500 and 50 cal yrs. BP, with colder pulses at 300, 180, and 100 cal yrs. BP ([Compagnucci, 2011](#)).

Moraines in the cirques of the Fuegian Andes have been identified and interpreted as a glacial expansion assigned to the LIA ([Rabassa et al., 1990; Coronato, 1994; Strelin et al., 2001; Planas et al., 2002; Menounos et al., 2013; Ponce et al., 2015](#)). The assignment of these moraines to the LIA (<1.0 ka) is based on their morphological and topographic differences with the moraines from the Late-Glacial, e.g., their fresh morphology and sub-rounded shapes, the formation of relative low ridges, their slightly consolidated sediments, their location near the current ice front, and the similarity of their positions with those of moraines in nearby regions previously assigned to LIA ([Strelin and Iturraspe, 2007; Strelin et al., 2008; Maurer et al., 2012](#)). [Ponce et al. \(2015\)](#) mapped LIA moraines in 26 cirque glaciers in the local Fuegian Andes, on average, at 680 ± 131 m a.m.s.l.

The LIA has not been clearly identified in the studied pollen records; however, fluctuations in the *Nothofagus* record for the last millennium have been associated to the LIA. In Las Cotorras peat bog (TLCo, 448 m a.m.s.l.), located in a hanging valley of the Fuegian Andes ([Fig. 1A](#)), the arboreal pollen recorded after 1000 cal yrs. BP, reached a minimum between 680 and 300 cal yrs. BP ([Borromei et al., 2010](#)). In Cañadón del Toro peat bog (TCT, 93 m a.m.s.l., [Fig. 1 B](#)), the pollen record showed a decrease in the frequency of *Nothofagus*, together with an increase in *Empetrum rubrum* towards 500 cal yrs. BP ([Borromei et al., 2016](#)). In TH (28 m a.m.s.l., [Fig. 1 A](#)), [Heusser \(1989\)](#) reported a decline in the pollen influx values of *Nothofagus* after 2350 yrs. BP, before 380 yrs. BP and recently; meanwhile at Bahía Franklin (IDE-2, 240 m a.m.s.l., [Fig. 1 A](#)), the pollen record shows a lower density of the *Nothofagus* forest between 500 and 50 cal yrs. BP in response to cold and dry conditions ([Ponce et al., 2017](#)).

In the central zone, the pollen record of TLC (208 m a.m.s.l.) and TTA (127 m a.m.s.l.) ([Fig. 1 A](#)), evidence a notable decrease in the frequency and concentration of arboreal pollen and an increase in *E. rubrum* after the last 1000 yrs and towards 400 cal yrs. BP, respectively. Both are indicative of a reduction in the *Nothofagus* forest under drier conditions ([Musotto et al., 2016](#)); similarly, the decline in Microthyriaceae and the record of *Glomus* sp. suggest local lower humidity during this period ([Musotto et al., 2017a](#)).

To the north, in the Fuegian steppe, the pollen records of LC and LLV show the development of shrubby vegetation and a decrease in grasslands in the last ca. 500 years, under low effective humidity. Likewise, the expansion of halophyte vegetation surrounding the shallow lakes, along with an increase in Zygnetaceae (*Spirogyna*) and low frequencies of *Pediastrum* and *Botryococcus braunii*, suggest a low lake water

level. The assemblage dominated by the ostracod *Limnocythere rionegrensis* Morph. II in LC ([Borromei et al., 2018](#)) and by the diatoms *Cocconeis placentula*, *Diploneis* sp., *Fragilaria brevistriata*, *Fragilaria construens* var. *venter*, *Fragilaria* sp2, *Hantzschia amphioxys*, *Hantzschia* sp., *Pinnularia borealis*, and *Thalassiosira patagonica* in LLV indicates brackish water conditions with seasonal fluctuations in the water level and desiccation processes ([Candel et al., 2020](#)). In turn, high sedimentation rates in the dunes of LLV, Laguna Perro (LP, [Fig. 1 A](#); [Montes et al., 2020](#)), and in AD suggest enhanced aridity in this period.

4.6. Tephra inputs from the Patagonian Andes

Throughout the Holocene, several ash deposition events from the volcanic fields located in the Andean Southern Volcanic Zone (SVZ; 33°–46° S) and in the Andean Austral Volcanic Zone (AVZ; 49°–55° S) were recorded ([Stern, 2008; Naranjo and Stern, 1998; McCulloch et al., 2005; Kilian et al., 2003; Wastegård et al., 2013](#)). The pioneering work of [Auer \(1958\)](#) in the Fuegian peat bogs proposed a sequence of three eruptive events (I, II, and III) since the beginning of peat bog formation inferring a different provenance for tephra II due to differences in color, thickness, and petrographic and geochemical composition in comparison with the other two tephras. More recent studies ([Unkel et al., 2008; Rabassa et al., 2009b; Borromei et al., 2010; Coronato et al., 2011; Musotto et al., 2016; 2017b](#)) recognized and date several tephra layers in sedimentary exposures or in peat and lacustrine cores. Based on the interpretation of their chemical signature, they were assigned to specific eruptions occurred in the Andean volcanoes along the Late Pleistocene-Holocene.

Regardless of sources and lapses, volcanic ash rainfall occurred several times during the Holocene and must be considered as important events of environmental changes in the Fuegian landscapes, mainly for soil composition changes and vegetation development.

Late Pleistocene tephra layers have been recorded in TLGB and TLCas, Isla de Los Estados by [Unkel et al. \(2008\)](#) and in central Tierra del Fuego ([Musotto et al., 2016, 2017b](#)) while Holocene ones were mentioned by [Coronato et al. \(2011\)](#) in Arturo dune and in several peat bogs of central and southern Tierra del Fuego ([Borromei et al., 2010, 2016; Vanneste et al., 2015; Musotto et al., 2016, 2017b; Savoretti, 2018](#)), in sedimentary cores of LF ([Waldmann et al., 2014](#)) and in Isla de los Estados ([Unkel et al., 2010](#)).

The Middle Holocene has been pointed out as the lapse in which an important event of ash rainfall occurred. It was well recorded in peat bogs of southern and central Tierra del Fuego ([Table 4](#)). The median probability of calibrated ages of 7254 cal yrs. BP was calculated by [Musotto et al. \(2016\)](#) at TLC as the minimum age for the eruption while the maximum median probability of calibrated age is 7992 cal yrs. BP at the same location ([Fig. 12](#)).

This eruption caused a drop in total pollen concentration values and the subsequent establishment of new habitats for pioneer plants, as shown by the pollen increase from *Gunnera*, *Gentiana*, and *Caltha* herbs and sedges. The fungal associations in TLC and TTA were characterized by a rise in the frequencies of chlamydospores of *Glomus* and hyphopodia of *Gaeumannomyces* sp., respectively, in relation with the development of grasslands and sedges during this event. In TLC, from 6300 cal yrs. BP and after an interval of ca. 1500 yrs., *Nothofagus* pollen increased, reaching pre-eruptive frequencies, and at 5300 cal yrs. BP, the forest adopted closed-canopy characteristics. In TTA, a lower impact on the arboreal vegetation was recorded, with its pre-eruptive relative values recovered at 7500 cal yrs. BP and the definitive physiognomy of the closed-canopy *Nothofagus* forest established at around 6500 cal yrs. BP ([Musotto et al., 2016, 2017b](#)). The Middle Holocene tephra dated into the above-mentioned range was also deposited in other peat bogs. In TH it was deposited between ca. 7100–7500 cal yrs. BP ([Vanneste et al., 2015; Savoretti, 2018](#)) causing a low concentration of woody components in the plant macrofossil record, whereas in TM, a tephra layer is recorded around 7700 cal yrs. BP ([Savoretti, 2018](#)). The decrease in the

Table 4

Previously published radiocarbon and calibrated ages for Middle Holocene tephra layers from southern and central peat-bogs in Tierra del Fuego.

Location	Sample depth (cm)	Laboratory code	Uncalibrated age (^{14}C yrs. B.P.)	$\delta^{13}\text{C}$ (‰)	Calibrated age yrs. B.P. (median probability)	1σ range	2σ range	Reference
Minimum ages (above tephra layer)								
TLC0	470–475	AA62823	7043 ± 47	-23,3	7839	7784–7873	7703–7938	Borromei et al., (2010)
TTA	553–554	AA86260	6881 ± 48	-26,5	7677	7614–7723	7581–7787	Musotto et al., (2017b)
TLC	247–248	AA83318	6410 ± 210	-27,2	7254	7152–7435	6785–7620	Musotto et al., (2016)
Maximum ages (below tephra layer)								
TTA	558–559	AA86259	7018 ± 46	-26,9	7812	7749–7861	7690–7876	Musotto et al., (2017b)
TLC	255–256	AA86263	7218 ± 48	-27,3	7992	7943–8023	7927–8050	Musotto et al., (2016)

Sphagnum magellanicum, and in woody vascular plants concentrations show an impoverished plant community after tephra deposition, accompanied by a slight increase in the concentrations of herbaceous vascular plants and macrofossils of roots, due to an unfavorable substrate for *Sphagnum* with excessive mineral nutrients. From 7100 cal yrs. BP, plant communities began to recover, but the peat bog was influenced by the presence of ash until ca. 6300 cal yrs. BP (Savoretti, 2018).

Borromei et al., (2010) recognized a Middle Holocene tephra layer deposited at the base of TLC0 (Fig. 1) core with the same geochemical composition of that of Hudson volcano (46°20'S/73° W) reported by Naranjo and Stern (1998) and by Stern (2008).

In the steppe, a tephra layer was recorded by Coronato et al. (2011) interbedded in the aeolian/paleosol succession exposed at the Arturo dune (DAr). Its geochemical signal shows the similarity in the $\text{SiO}_2/\text{K}_2\text{O}$ ratio of the Mt. Burney volcano (VMB, 52° 18'S) ashes, as it was presented by Stern (2008). Unfortunately, not a precise date is available due to its deposition in a 6.9 m thick aeolian, but the underlying and overlying paleosols were dated between 6650 and 4948 cal yrs. BP (Table 3).

4.7. The recent warming

Studies carried out in glaciers of the Southern Patagonian Andes show a general retreat trend since the LIA, accelerated over the last five decades (Masiokas et al., 2009a, 2009b; Davies and Glasser, 2012; Rivera et al., 2012; Falaschi et al., 2013; Meier et al., 2018). This trend is attributed mainly, and in most cases, to a climate change characterized by an increase in air temperature and an apparent decrease in rainfall (Glasser et al., 2004; Aniya, 2013; Falaschi et al., 2019). A similar behavior has been observed in glaciers in the Argentine sector of the Fuegian Andes (Strelin and Iturraspe, 2007; Iturraspe, 2011). Ponce et al. (2015) calculated a retreat magnitude of the Fuegian Andes cirque glaciers of 778 ± 432 m from their maximum position in the LIA to the present. This is approximately equivalent to a reduction of $41 \pm 23\%$ of its surface and explains the wide variability of distances in the different topographic conditions of the studied cirques. Studies conducted on glaciers located in the Martial range (MR, Fig. 1 B) indicate relative stability of their fronts from the LIA until 1943 AD, followed by a slow retreat until 1957 AD, a new stabilization towards 1970 AD, and finally a continuous and accelerated retreat during the first decade of 21st century (Strelin and Iturraspe, 2007). A similar behavior over the last five decades was reported for Chato Glacier (GCh, Fig. 1 B), located in the western sector of Martial range (San Martín et al., 2021b), and other Fuegian Andes glaciers.

The speed at which the cirque glaciers of the Fuegian Andes have retreated since the LIA is associated with changes in air temperature and precipitation recorded by meteorological stations in the city of Ushuaia (Fig. 1 B) since 1902 AD. These data show a decrease in the mean annual

temperature curve between 1922 and 1950 and a decrease in rainfall since 1939 AD, after at least 10 years of hydric excess. Between 1951 and 1956 AD, higher mean annual temperatures were recorded within a general trend of lower mean annual temperatures. Since 1970 AD, the annual mean temperature curve has almost continuously risen, while the precipitation trend curve has diminished (San Martín et al., 2021b).

The relative frequency values of the pollen records of TLC, TTA, TCT, and TLC0 peat bogs, located in the center-south of Tierra del Fuego, as well as IDE-1 and IDE-2 peat bogs in Bahía Franklin, southwest of IDE, show a rapid increase in arboreal pollen after the minimum values reached during the LIA, together with a decrease in dwarf shrub heath (Ericaceae), scrub (Asteraceae subf. Asteroideae), and grass (Poaceae) vegetation (Borromei et al., 2010, 2016; Ponce et al., 2011, 2017; Musotto et al., 2016, 2017b). In TH, Savoretti (2018) recorded a significant drop in the concentration of *Sphagnum magellanicum* between 200 and 100 cal yrs. BP interpreted as the occurrence of a less cold and dry climatic conditions, whereas TM (Fig. 1 A) displays an increment in the concentration and diversity of liverworts and a decrease in mosses and vascular plants (Savoretti, 2018).

5. Discussion

The integration of various paleoenvironmental studies in the Argentinian sector of IGTDF and IDE is essential to the reconstruction of the Holocene environmental history of the southernmost portion of South America. In this way, it is possible to contextualize it within the regional, hemispheric, and global climate evolution and to compare it with simulations from climate models. However, when paleoenvironmental records were obtained with different sampling resolution and time spans, their comparison or correlation not always give the same signals. On the one hand, the Fuegian insular environment is strongly influenced by latitude, winds, and the arrangement of orographic barriers but also by the local characteristics of each studied environment. Besides, the information provided by the different proxies depends on their sensitivity and threshold to climate change, and non-linear proxy-climate relationships are frequent (Kilian and Lamy, 2012). For this reason, different paleoenvironmental records and different timespans do not always reflect the same signal to climate change. A paleoclimatic correlation of the Argentinian sector of IGTDF and IDE with southern Patagonia and Antarctica localities based on selected proxies and localities is presented (Fig. 12).

5.1. Early to Middle Holocene

Patches of *Nothofagus* forest and steppe vegetation dominated the southern Argentinian IGTDF and IDE landscape during the Late Glacial-Holocene transition (Fig. 12 I, J, K and L). Trees began to expand and colonize the areas previously occupied by the gramineous/shrubby

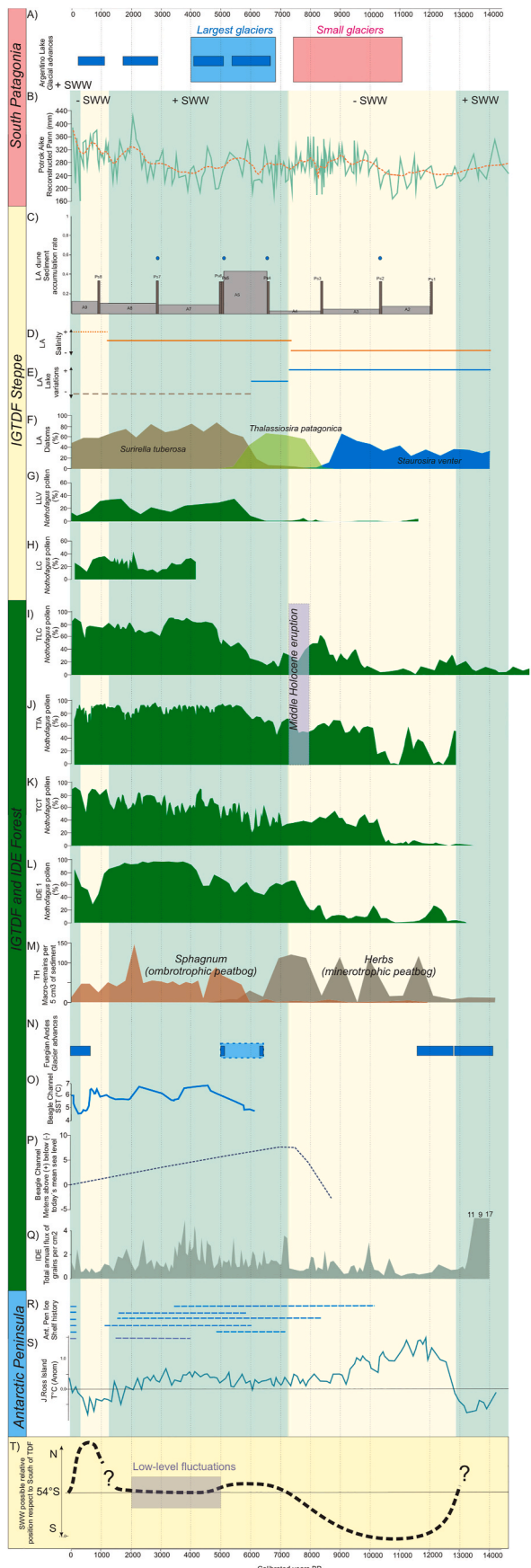
vegetation ca. 10,500 cal yrs. BP, being analogous to the current landscape of the *Nothofagus* forest-steppe ecotone. In addition, the record of arbuscular mycorrhizal and coprophilous fungi allows us to infer the presence of grasslands and herbivorous animals in the peat bogs during this period. A similar vegetation pattern has been reported by other authors for localities in the Argentinian sector of IGTDF (Markgraf and Huber, 2010; Fontana and Bennett, 2012; Mansilla et al., 2018; McCulloch et al., 2020). Although no charcoal analysis was performed, the record of dryland/fire fungi indicators in the pollen spectra at TLC and TTA (Musotto et al., 2016, 2017b), were probably related with regional fire events (Heusser, 2003; Whitlock et al., 2007; Markgraf and Huber, 2010). The expansion of *Nothofagus* from multiple ice-free refuges was not synchronous and possibly was conditioned by the altitudinal gradient, the topographic characteristics, and the soil type, as well as by the W-E and N-S precipitation gradients. The gradual expansion of forest communities in the south of Argentinian IGTDF and the development of minerotrophic peat bogs seem to coincide with the gradual decrease in temperature in the Antarctic Peninsula (PA, Fig. 12 S), after the Holocene Thermal Maximum, which started around 11,500 cal yrs. BP (Mulvaney et al., 2012) and with the low intensity of the SWW in these latitudes (Fig. 11Q) according to Björck et al. (2012) and Vanneste et al. (2015). This would have provoked a gradual and oscillating migration of the SWW belt core from Antarctic latitudes towards the

south of IGTDF (Fig. 12 T). At Cipreses lake (LCi, 51° S, Fig. 1 C), Moreno et al. (2018) also pointed out an increase in *Nothofagus* pollen and its hemiparasite *Misodendrum*, resulting in the establishment of the closed-canopy Magellanic forest, which suggests gradual warming under humid conditions between 12,700–11,000 cal yrs. BP.

The environmental stability deduced from the development of the three paleosols of aeolian origin in LA (Fig. 12 C) during the Late Glacial-Holocene transition and the Early Holocene is consistent with a relative low intensity of SWW in favor of humid air masses reaching the north of IGTDF from the South Atlantic. According to Coronato et al. (2011, 2021), this environmental stability denotes a decrease in wind activity favoring pedogenesis, together with the low rate of accumulation of aeolian sediments in DA between Ps1, Ps2, and Ps3 (Fig. 12 C) developed between 12,800–8300 cal yrs. BP (Table 3). Pedological characteristics of these paleosols indicate lower relative aridity or higher air temperature in comparison with the paleosols developed during the Middle-Late Holocene; in addition, Ps2 has been described as an indicator of a relative rise in rainfall (Orgeira et al., 2012). The low intensity of SWW during this period is also reflected in the *Myriophyllum* record in the LA core, since it indicates a water body with low inorganic turbidity and high-water availability and, therefore, a lower impact of the wind on the surface of the shallow lake (Fernández et al., 2020). Shallow lake phases I to III may have developed during this period, with the greatest relative



Fig. 11. Tephra layers deposited in peat cores and aeolian exposures. A) Late Pleistocene tephra layer at La Correntina peat bog. B-D) Middle Holocene tephra at three different peat bogs, B) La Correntina, C) Terra Australis, D) Moat. E-F): Middle Holocene tephra of 6 cm depth into Arturo Dune aeolian sequence. G-H: tephra layer deposited into the Amalia Dune aeolian sequence, probably the same of Arturo Dune one, based on color and texture and chronostratigraphy (after Coronato et al., 2021).



(caption on next column)

Fig. 12. Simplified diagrams from our results and several ones from the literature comparing the behavior of selected proxies along 14 ka calibrated yrs. BP. The vertical bars which cross most of the figure (from B to S) indicate low SWW (yellow bars) and high SWW (green bars) intensity. A) Argentino Lake (N° 6 in Fig. 1 C) glacial advances (modified from Kaplan et al., 2016). B) Reconstructed paleoprecipitation at Potrok Aike Lake (N° 7 in Fig. 1 C) (Schäbitz et al., 2013). C) Arturo Dune (N° 15 in Fig. 1 A) sediment accumulation rate. D) Arturo Lake (N° 1 in Fig. 1 A) salinity variations (Laprida et al., 2021). E) Arturo Lake water-level variations (Fernández et al., 2020). F) Arturo Lake diatoms percentage *Surirella tuberosa*, *Thalassiosira patagonica*, *Staurosira venter* (Fernández et al., 2020). G) Las Vueltas Lake (N° 3 in Fig. 1 A) *Nothofagus* sp. Pollen percentage (Candel et al., 2020). H) Carmen Lake (N° 4 in Fig. 1 A) *Nothofagus* sp. Pollen percentage (Borromei et al., 2018). I) La Correntina (N° 4 in Fig. 1 A) peat bog *Nothofagus* sp. Pollen percentage (Musotto et al., 2016). J) Terra Australis (N° 3 in Fig. 1 A) peat bog *Nothofagus* sp. pollen percentage (Musotto et al., 2017b). K) Cañadón del Toro (N° 6 in Fig. 1 A) peat bog *Nothofagus* sp. Pollen percentage (Borromei et al., 2016). L) IDE-1 (N° 9 in Fig. 1 A) peat bog *Nothofagus* sp. Pollen percentage (Ponce et al., 2011). M) Harberton (N° 2 in Fig. 1 A) peat bog *Sphagnum* and herbs concentrations (Savoretti, 2018). N) Fuegian Andes glacier advances (modified from Menounos et al., 2013). O) Beagle Channel (Fig. 1 B) sea surface temperature (SST) from Obelic et al. (1998). P) BC Holocene sea level curve (Björck et al., 2021). Q) IDE total annual flux of grains (Björck et al., 2012). R) Periods of open marine conditions in Prince Gustav Channel (light blue) and Larsen A (grey) ice shelves of Antarctic Peninsula (Mulvaney et al., 2012). S) Temperature anomaly record from James Ross Island ice core (Mulvaney et al., 2012). T) Tentative and relative Southern Westerly Winds (SWW) position respect to 54°S.

slopes and a great lake surface compared with the present-day surface (Table 3). This situation coincides to the development of higher paleoshoreline levels and relative low salinities in Cardiel lake (49° S, LCar, Fig. 1 C), according to Stine and Stine (1990) and Ariztegui et al. (2008), and with the ostracod assemblages dominated by *Limnocythere patagonica* (Ramos et al., 2019). These humid conditions were also recorded in Potrok Aike lake (LPA, Fig. 1 C) and other localities in southern Patagonia (Haberzettl et al., 2007; Horta et al., 2011; Franco et al., 2016). The precipitation model for Potrok Aike lake (LPA, Fig. 12 B), in Extra-Andean Patagonia, indicates higher precipitation from the beginning of the Early Holocene to ca. 8000 cal yrs. BP (Schäbitz et al., 2013). These signals correspond to the conceptual diagram of Quade and Kaplan (2017) for latitude 50° S.

A decrease in the intensity of the SWW during the Early Holocene under warm and dry conditions, known as Extended Warm Dry Anomaly (EWDA), as proposed by Moreno et al. (2018, 2021), has been indicated for other regions of Patagonia, suggesting the influence of an extended negative anomaly of the SWW at 52° - 54° S (Moreno et al., 2018, 2021). Furthermore, Irurzun et al., 2014 propose a sedimentary stratification of LPA during at least four intervals during the Early Holocene related with a weakening of the SWW. This diminished intensity seems to coincide with a minimum glacier extent in Argentino lake (LArg) basin (Kaplan et al., 2016, Figs. 1 C and Fig. 12 A).

McCulloch et al. (2020) reported a sustained period of drier conditions between 9700 and 6000 cal yrs. BP on Navarino island (Fig. 1 A), which would have generated a contraction in the forest communities. According to these authors, the reduction in effective humidity suggests a weaker influence of the SWW, due to the extreme migration of the wind belt towards polar latitudes. In TLC (Fig. 12 I) and LL, Musotto et al. (2016) and Mansilla et al. (2018) registered a decreased frequency of *Nothofagus* between ca. 8600-6500 cal yrs. BP. In the Fuegian steppe, according to Fernández et al. (2020), the predominance in LA of the diatom *Thalassiosira patagonica* and the ostracod *Limnocythere rionegroensis*, typical of slightly brackish and alkaline waters, suggest relatively low water level (Fig. 11 E) between ca. 8500-6000 cal yrs. BP (Fig. 12 F). In addition, between 8300 and 6500 cal yrs. B.P., Arturo dune exhibits the lowest aeolian sediment accumulation rate in the entire sedimentary sequence (A4, Fig. 12 C). These arid conditions coincide with the decrease in rainfall recorded by Schäbitz et al. (2013) in LPA

around 8000 cal yrs. BP (Fig. 12 B).

In the marine ecosystems, one of the most significant environmental changes implied the seawater-flooded lowlands which also meant the spatial redistribution of the region's canoe peoples (Zangrandino et al., 2016). The earliest evidence dates back to the Early-Middle Holocene. The glacio-isostatic model on the south coast of CB in Navarino Island, indicates a rapid relative rise in sea level between ca. 8500-6500 cal yrs. BP, with a maximum between 7500 and 7000 cal yrs. BP, followed by a slow relative drop (Björck et al., 2021, Fig. 12P). After that, successive levels of beach, coastal ridges, tombolos, and inlets were formed with estuarine dynamics on both channel coasts and islands. According to our evidence, the oldest outcropping sediments, located in BL and AS sites (Fig. 1 B), is ca. 8300 cal yrs. BP (Rabassa et al., 1986, 2009a; Candel et al., 2018). Besides, marine deposits from ca. 8600 cal yrs. BP were identified in Caleta Eugenia (McCulloch et al., 2019), on the southern coast of the eastern end of the channel (CE, Fig. 1 A). On the Atlantic coast, our evidence indicates that the entry of seawater reached a maximum between ca. 8500-6000 cal yrs. BP with the development of a coastal lagoon in LLV and paleobays, paleocliffs, barriers, littoral ridges, and paleomarshes along the entire coast (Isla and Bujalesky, 2000; Bujalesky, 2007; Montes et al., 2018, 2020; Candel et al., 2020).

The volcanic activity in the southern Patagonian Andes during the Early-Middle Holocene (Stern, 2008; McCulloch et al., 2005, Wastegård et al., 2013) caused several ash deposition events (Fig. 12 C, I, J, K), affecting terrestrial plant communities and aquatic ecosystems (Musotto et al., 2016, 2017b; Savoretti, 2018; Fernández et al., 2020) and probably the terrestrial fauna communities and the human groups that inhabited the region. According to Rabassa et al. (2009b), in Tierra del Fuego, tephra deposits are preserved in different sedimentary environments and different times.

5.2. Middle to Late Holocene wet-dry oscillations

In the south of the Argentinian sector of IGTDF and IDE, both the *Nothofagus* pollen and plant macrofossils records from peat bogs indicate an increase in effective humidity and cold conditions from ca. 6700 cal yrs. BP, which would have led to the expansion of the closed-canopy *Nothofagus* forest and a change in the hydrological conditions, favoring the development of ombrotrophic *Sphagnum* peat bogs (Fig. 11 I, J, K, L, M). Similar conditions have been observed in other IGTDF locations (Markgraf and Huber, 2010; Mansilla et al., 2018; McCulloch et al., 2020) and southern Patagonia (Villa-Martínez and Moreno, 2007; Moreno et al., 2018). The expansion of the *Nothofagus* forest limit towards the steppe is observed in the LLV pollen record after 6000 cal yrs. BP (Fig. 12 G), when the extra-local arboreal pollen frequency values rose remarkably (Candel et al., 2020). This is corroborated by the LC pollen record (Fig. 12 H), which points to an increase in the *Nothofagus* frequencies at ca. 4000 cal yrs. BP (Borromei et al., 2018). The development and expansion of the longitudinal forest margin towards the NE under higher humidity conditions may be linked to an increase in the intensity of the SWW proposed by Björck et al. (2012, Fig. 11 Q), possibly associated with the core migration of the SWW belt towards 54°-55°S from Antarctic latitudes (Fig. 12 T).

During this forest expansion stage, intervals of low *Nothofagus* pollen input between 6380 and 5000 cal yrs. BP in TH (Heusser, 1989) and between 6310 and 4510 cal yrs. BP in Ushuaia 2 peat bog (TU2, Fig. 1A) (Heusser, 1998) and a decrease in the concentration values at ca. 6800 cal yrs. BP and between 5000 and 4500 cal yrs. BP in IDE-1 (Ponce et al., 2011) were observed. These intervals could be associated with the 'Neoglacial' cold climate event proposed by Kaplan et al. (2016) for the Argentino lake basin (Fig. 12 A), by Menounos et al. (2013) for the Fuegian Andes (Fig. 12 N), between 6100–4500 and 5300-5000 cal yrs. BP and by Reynhout et al. (2019) in Torre Glacier (49° S-57° W) at 6100 and 4200 cal yrs. BP. Simultaneous glacial advances were recorded east of PA, in James Ross Island (Fig. 12 S) around 5400-4800 cal yrs. BP and at 4200 cal yrs. BP by Hall (2009) and 5000-4000 cal yrs. BP by Kaplan

et al. (2020). The paleotemperature curve of the Beagle Channel (Fig. 12 O), based on a $\delta^{18}\text{O}$ record from *Mytilus edulis* shells collected from archeological sites (Obelic et al., 1998) and from elevated marine beaches dated ca. 5100 cal yrs. BP (Gordillo et al., 2014), shows relative low temperatures between 6000 and 5000 cal yrs. BP. According to Strelin et al. (2008), periods of cold sea temperatures during the Late Holocene promoted favorable climatic conditions for the expansion of alpine glaciers in southern Tierra del Fuego. For the same period, the paleotemperature curve of Mulvaney et al. (2012) for PA shows a slight thermal decrease (Fig. 12 R). The high humidity inferred from the region's pollen data supports the interpretation that, during the Neoglacial advances proposed by Menounos et al. (2013), the SWW were located slightly north of 54–55°S. This position of the SWW would have allowed a greater influence of the winds from Antarctica in the south of IGTDF, creating slightly colder and thus favorable conditions for glacier advance.

The pollen records analyzed here show the highest development of the closed-canopy *Nothofagus* forest between ca. 5500-3000 cal yrs. BP (Fig. 11 I and L) under humid and cold conditions. However, in the BC, an increase is observed in the paleotemperature curve during this period (Obelic et al., 1998, Fig. 12 O). In addition, the paleotemperature curve of Mulvaney et al. (2012) indicates temperatures slightly higher than the current ones between 5000 and 2000 cal yrs. BP (Fig. 12 S), with a remarkable reduction in Prince Gustav and Larsen A ice shelves, located northeast of PA. This increase in temperatures coincides with a rise in the intensity of the SWW (Björck et al., 2012, Fig. 12 Q). This evidence suggests that the SWW belt core could have been re-established at 54°-55°S during this time interval (Ponce et al., 2011; Björck et al., 2012) with a maximum intensity ca. 3800 cal yrs. BP (Fig. 12 T). The analysis of the malacofauna of the BC and its isotopic signal (Fig. 12 O) indicates a period of warmer conditions and higher productivity between ca. 4500-3000 cal yrs. BP (Gordillo et al., 2015; Obelic et al., 1998) compared with the rest of the Holocene. These could be attributed to a greater input of micronutrients to the marine system as a result of precipitation and the discharge of freshwater from the adjacent mountain ranges towards the continental margin (Gordillo et al., 1993; Candel et al., 2009; Candel and Borromei, 2013). Also, in RO (Fig. 1 B), between 3900 and 3800 cal yrs. BP, the bloom of opportunistic dinoflagellate cyst and the increase in fresh to brackish water algae reveal a greater input of surface runoff to the marine environment (Candel and Borromei, 2013, 2016). This climatic improvement is comparable to the Late Holocene Warm Dry Period (LHWDP) identified in LCI (Moreno et al., 2018) and a to a short warming period between ca. 4000-3000 BP in PA (Strelin et al., 2006; Etourneau et al., 2013). The geomorphological conditions, depth, and sediment variations in the BC gave rise to heterogeneous habitats that facilitated the development of diverse local benthic communities. Settled in the different patches, these paleocommunities changed their arrangement during the Holocene (Gordillo et al., 2013), according to the hydrological and substrate shifts taking place in the channel, forming a dynamic mosaic model, which was also identified in San Matías gulf (Fig. 1 C), in Northern Patagonia (Bayer et al., 2016).

In the Fuegian steppe, the intensification of the SWW would have generated drier conditions in response to a steepening of the precipitation gradient. In LA, intensification of the wind and aridity, increased salinity and a decrease in the water level are inferred from 6000 cal yrs. BP (Fig. 11 D, E and F), based on the alga-diatom-ostracod record (Fernández et al., 2020). Besides, the LA dune registered a rise in the sediment accumulation rate towards 6500 cal yrs. BP after the development of Ps4 (Fig. 12 C). Extra-Andean Patagonia experienced a decrease in precipitation values between 5500 and 2500 cal yrs. BP (Schäbitz et al., 2013, Fig. 12 B), in coincidence with the major increase in the intensity of the Westerlies recorded for IDE (Björck et al., 2012, Fig. 12 Q). Similarly, the lake levels of the Extra-Andean Patagonian lakes responded with gradual decreases in the water level (Ariztegui et al., 2008) or were subject to lower humidity intervals (Franco et al., 2016; Ramos et al., 2019) and intensified drying due to the wind effect.

The paleosol sequences preserved in the perched dunes (Coronato et al., 2021) show alternating conditions of major availability of effective humidity and aridity within a general trend towards arid conditions. In addition to the inferred changes in surface and depth variations (Table 2, Fig. 12 E), alternation of wet-dry periods has also been detected in the shallow lakes (Borromei et al., 2018; Fernández et al., 2020; Laprida et al., 2021), some of them lasting hundreds of years. For LCi, Moreno et al. (2018) interpreted nine positive Southern Annular Mode-like (SAM) events equivalent to warm-dry intervals at centennial timescale from 5800 cal yrs. BP, alternating with cold-wet intervals or negative SAM-like states favoring glacier expansion. These variations could be associated with high-frequency changes and low amplitude in the intensity of the SWW. Some levels of the aeolian deposit and paleosol sequences preserved in the perched dunes of the Fuegian steppe during this period could be a response to these SAM events.

Although the pollen records presented here for the forest area in southern Argentinian IGTDF and IDE do not reflect centennial climate variability during the Middle and Late Holocene, an increase in variability after ca. 5900 cal yrs. BP was observed on Navarino Island by McCulloch et al. (2020) due to a reduction in mire surface wetness. The authors identified five periods of rapid climate change leading to drier conditions. Minor climatic changes are also reflected in the high variability in the SWW intensity recorded in IDE since 6500 cal yrs. BP (Björck et al., 2012, Fig. 12 Q). This would indicate that, despite the variations of minor magnitude in the position of the SWW between 5000 and 1000 cal yrs. BP, the SWW belt core would have remained between 54° and 55°S, leading to conditions of high effective moisture in the forest area of the Argentinian IGTDF and IDE (Musotto et al., 2017b; Ponce et al., 2011). From 3000 cal yrs. BP, the SWW weakened (Björck et al., 2012, Fig. 12 Q) and, subsequently, the temperature of the eastern sector of PA diminished after 2500 cal yrs. BP (Mulvaney et al., 2012, Fig. 12 S), while the sea surface water temperature decreased in the BC from 2300 cal yrs. BP (Obelic et al., 1998, Fig. 12 O). These changes coincide with a sharp drop in the *Nothofagus* pollen concentration in IDE (Ponce et al., 2011) and in their relative frequencies in TLC (Musotto et al., 2016, Fig. 12 I), suggesting drier conditions. The shallow lakes of the steppe experienced humid intervals associated with the input of humid air from the Atlantic Ocean, coinciding with the observed trend towards a rainfall increase in LPA, Extra-Andean Patagonia, from 2500 cal yrs. BP (Schäbitz et al., 2013, Fig. 11 B). This condition could have favored the development of paleosols in the perched dunes of the Fuegian steppe between 2000 and 1000 cal yrs. BP (Coronato et al., 2021, Fig. 12 C).

5.3. Last 1000 cal yrs. BP

One of the global climate changes detected in the last millennium is a warming trend between 1100 and 900 cal yrs. BP (Compagnucci, 2011), recorded also in several sites of Patagonia (Favier Dubois, 2007; Stoessel et al., 2008, among others). In LCi, the MCA was correlated with a warm and dry event corresponding to the penultimate positive SAM-like event, registered between 1000 and 700 cal yrs. BP and related to a weakening and migration of SWW southwards (Moreno et al., 2018). Warm and dry climatic conditions have only been reported for some peat bogs in the Fuegian Andes (Mauquoy et al., 2004; Savoretti et al., 2017) owing to a decrease in iron content in the sedimentary record of LF (Waldmann et al., 2010). In the Beagle Channel, the existence of MCA was inferred from the rise in seawater temperature between 800 and 500 cal yrs. BP (Obelic et al., 1998, Fig. 11 O). However, not all the proxies recorded this warming in IGTDF. The temperature increases and the drier conditions defined for the MCA may not have been intense enough to cause a significant change in the *Nothofagus* forest, since the MCA was not identified in our pollen records for the south of IGTDF and IDE. In this sense, Reynhout et al. (2021) mentioned an out-of-phase glacial advance occurred within the Cordillera Darwin at 870 cal yrs. BP linked to a southerly shift or enhanced westerly flow that resulted in increased

cloudiness and precipitation over Tierra del Fuego. While the seawater paleotemperature curve for western PA (Shevenell et al., 2011) shows a warming trend between 1600 and 400 cal yrs. BP, the records of Mulvaney et al. (2012) indicate that the PA did not experience significant warming during the MCA (Fig. 12 S). However, pedogenetic events that began around 1000 cal yrs. BP in both, northern IGTDF and southern Patagonia (Favier Dubois, 2003, 2007) could be related with the MCA.

In the perched dune of LA, paleosol Ps8 (Fig. 12 C) is located within the time range corresponding to the MCA. The reconstruction of paleoprecipitation in southeastern Extra-Andean Patagonia (Fig. 12 B) shows a rise between 1300 and 300 cal yrs. BP (Schäbitz et al., 2013), related with the advection of humid air masses from the South Atlantic due to the weakening of the SWW.

The cold event of the last millennium is associated with the last regional glacier advance, assigned to the LIA. Moreno et al. (2018) reported cold and humid conditions between 600 and 200 cal yrs. BP at 51°S during a negative SAM-like event related to a northward expansion of the SWW belt. By contrast, Echeverría et al. (2017) point out cold and dry conditions during the LIA, also linked to northwards migration of the SWW and equally affecting forest and steppe environments between 48° and 52°S. This environmental situation is contemporaneous with the generation of moraines in Argentino lake basin before 400 and after 300 cal yrs. BP (Strelin et al., 2014) or around 360-240 cal yrs. BP (Kaplan et al., 2016, Fig. 12 A).

According to geomorphological evidence obtained from cirque glaciers in the Fuegian Andes and according to Menounos et al. (2013, Fig. 12 N), the LIA was the most widely spread Neoglacial advance in the Argentinian sector of IGTDF. The paleotemperature curve proposed by Obelic et al. (1998, Fig. 12 O) reveals a significant cooling period between 500 and 50 cal yrs. BP, mainly between 300 and 200 cal yrs. BP. During this period, the BC waters would have registered the lowest temperatures in the last 6000 years, with negative anomalies close to 1.4 °C (Fig. 12 O). The analysis of growth increments and oxygen isotope from bivalve shells from the BC also indicate a cooling at ca. 500 cal yrs. BP (Gordillo et al., 2015). This coincides with the pollen records studied in the south of IGTDF and IDE (Fig. 12 I, J, K and L) which indicate cold conditions and low effective humidity between 600 and 50 cal yrs. BP leading to decrease in the frequencies and concentrations of arboreal pollen (Ponce et al., 2017). In IDE, a lower intensity of the SWW between 1000 and 300 cal yrs. BP was inferred (Björck et al., 2012, Fig. 12 Q). In addition, McCulloch et al. (2020) recorded a reduction in forest cover and a decrease in pollen preservation on Navarino island after 1000 cal yrs. BP, reflecting cold and dry conditions.

The SWW migration to lower latitudes (Fig. 12 T) could have allowed the Polar Front to exert a great influence on the south of IGTDF, allowing the advection dry and cold air masses (Schneider et al., 2003). The reduction in the intensity of SWW in IGTDF and IDE is reflected in the low input of extra-regional pollen in the pollen records of the Fuegian steppe around 500 cal yrs. BP (Fig. 12 G and H). In Extra-Andean Patagonia, the precipitation fell down around 300 cal yrs. BP (Schäbitz et al., 2013, Fig. 11 B) due to strengthening of the SWW. However, Xia et al. (2018) indicated that weaker SWW and more frequent easterly flows would have enhanced moisture supply from the Atlantic Ocean in southernmost Patagonia (54° S) during this period.

In the eastern sector of PA, Mulvaney et al. (2012) observed a significant cooling period between 1500 and 100 cal yrs. BP (Fig. 12 S), reaching the lowest temperatures of the entire Holocene around 500 cal yrs. BP. This also coincides with a period when the ice shelves in eastern PA grew and stabilized. In western PA, the seawater became cooler between 400 and 150 cal yrs. BP (Shevenell et al., 2011).

Over the last 500 cal yrs. BP, the relative frequencies of *Nothofagus* pollen have risen in all the localities studied, while PA (Shevenell et al., 2011) and Beagle Channel seawater temperatures have increased (Obelic et al., 1998, Fig. 12 O). The forest recovery also coincides with a slight increment in the SWW intensity registered in IDE (Björck et al., 2012, Fig. 12 Q), also reflected in a rise in extra-regional pollen in the

localities of the Fuegian steppe (Fig. 12 G and H).

Besides, the *Sphagnum* cover in the peat bogs on the northern coast of the BC (TH and TM) has diminished (Fig. 12 M), and the diversity of vegetation (lichens, liverworts, *Empetrum rubrum* shrubs) has grown over the last 200 years, suggesting drier surface conditions, although the influence of anthropic activity since the mid-20th century as an agent of environmental disturbance cannot be ruled out. Dendrochronological records from southern Patagonia reveal a long period of cold years between 1640–1850 AD, followed by warming trend in air temperature with maximum in the 1980s AD (Roig and Villalba, 2008). Although the authors indicate remarkable cold events in the 1650s AD, 1660s AD, 1690s AD, 1700s AD, 1810s AD, and 1850s AD, these events are not reflected in the dynamics of the Fuegian forest from the pollen records.

Since the 20th century, there has been a trend towards rising temperatures (Roig and Villalba, 2008) and decreasing rainfall (San Martín et al., 2021b), along with the marked retreat of the cirque glaciers in the Argentine sector of the Fuegian Andes, particularly over the last five decades (Strelin and Iturraspe, 2007; San Martín et al., 2021b). This regional thermal increase has led to the drying out of shallow lakes in the Fuegian steppe, resulting in deflation processes, formation of wind mantles (Villarreal et al., 2014), and lunette and nebka dune fields (Coronato et al., 2012).

According to Moreno et al. (2014, 2018), the current situation of the SWW in the positive SAM phase or displacement towards polar latitudes is reflected in rising temperatures, reduced glacier size, dry lakes, the formation of dust mantles and dunes in Tierra del Fuego, coinciding with the rise in temperature and the collapse of the ice shelves in PA.

6. Final remarks

Do to their latitudinal position between Patagonia and Antarctica, IGTDF and IDE (53° – 55° S) are key regions to reconstruct SWW mobility and intensity throughout the Holocene. Furthermore, the insular character and the presence of two well-defined bioclimatic regions such as the *Nothofagus* forest and the steppe made it possible to analyze distinct responses of terrestrial and aquatic environments to changes in SWW.

The results obtained from the studied proxies show some discrepancies in the air circulation model in Tierra del Fuego when comparing to Patagonia, or even a lack of synchronization. The first, is a compatible situation with the current differences' climatic conditions among Tierra del Fuego and central and northern Patagonia; the lack of synchronization could be probably related to different record resolution derived from intervals of sampling and dating used in the analyzed papers. Besides, different environment changes and responds to external factors at different rates, showing different abilities to recover from disturbances and resolve events accurately in time because of the archives' inherent attributes. Additionally, each proxy type reflects its idiosyncratic sensitivity and critical threshold in responding to changes in different climatic parameters. Moreover, some proxies have non-linear responses, especially when critical thresholds are exceeded. For these reasons, it is not always possible to observe the same signal and intensity to climate change when different paleoenvironmental records and/or proxies are compared or correlated.

However, our integrated results allow us to establish some general trends regarding the climatic history of IGTDF and IDE. In general, it is observed that the greater intensity of the SWW is associated with the greater moisture input to the IGTDF and IDE forests and the wider rainfall gradient, leading to windy and arid conditions in the steppe zones. In contrast, the lower intensity of the SWW caused a lower moisture input in the forests, favoring the entry of humid air from the Atlantic Ocean and promoting humid and less windy conditions in the steppe. The limitations imposed by some proxies do not make it possible to clearly identify smaller environmental variations.

During the Early to Middle Holocene, the positioning of the SWW south of IGTDF resulted in low wind intensity and higher than the current temperatures. In the southern zone of IGTDF and IDE, these

conditions favored the gradual expansion of forest communities and the development of minerotrophic peat bogs while in the steppe zone, higher humidity and less windy conditions to the establishment of larger and deeper than present-day shallow lakes and the onset of pedogenetic processes in former aeolian deposits.

During the Middle Holocene, the analysis of situation shows that the gradual migration of the SWW core from Antarctic latitudes towards 54° – 55° S enhanced the wind intensity, generating humid conditions in the forest and aridity and windy conditions in the steppe, possibly under a less cold climate than the current one. These conditions favored the establishment of a closed-canopy forest and the ombrotropic peat bogs. The greatest forest development occurred between 5000 and 3000 yrs. BP during the phase of highest humidity and wind intensity, possibly resulting from the northern shift of the SWW core in the region. The forest retreated in southern IGTDF after 3000 yrs BP is consistent with the weakening of the SWW and a cooling phase of the BC water. In the steppe, the windy conditions substantially changed the hydrology of the shallow lakes, giving rise to a drying phase that continues to the present day, coinciding with high sedimentation rates in the aeolian environments. In this area, centennial environmental oscillations alternated between humid and arid conditions, within a general trend to aridization.

Since 1000 cal yrs BP, a significant climate change is observed in the region, possibly related to the LIA event. However, there is no clear evidence demonstrating the occurrence of MCA warming. The positioning of the SWW core to the north of IGTDF caused its weakening in the region and the decrease in the BC water temperatures. This process led to the forest retreat and the glacier expansion in the south; in contrast, no clear evidence of LIA cooling is observed in the steppe zone of the Argentinian sector of IGTDF.

After 500–300 cal yrs. BP the forest has recovered in coincidence with a slight increase in SWW and the water temperature in the BC due to the migration of the SWW belt towards Antarctic latitudes. In the steppe zone, these conditions continued to cause aridity, salinization, and finally, seasonal drying of the shallow lakes, as well as high sedimentation rates in aeolian deposits. This warming trend was reinforced since the middle of the 20th century, as shown by a marked retreat of the cirque glaciers.

Other environmental events occurring in the Middle Holocene involve drivers unrelated to the variability of SWW. The marine transgression that occupied troughs, fjords, and depressions caused a significant change in the spatial configuration of the Argentine side of IGTDF and nearby islands, creating landforms and littoral environments colonized by a great heterogeneity of local microplanktonic and benthic communities similar to the current ones and with species that still live in the channel. Moreover, tephras were formed due to the arrival of dispersed pyroclastic material towards the SW during several Andean volcanic eruptions during the Late Glacial and the Middle Holocene, causing paleoecological shifts in peat bogs and changes in the trophic state of aquatic environments.

Our results show similar environmental trends in the center and south of the Argentinian sector of IGTDF, IDE, and PA, both in terrestrial and marine environments, as well as the steppe zone and Extra-Andean Patagonia. The integration of the paleoenvironmental results presented here highlights the importance of this sector of southern South America as a region of great biodiversity remarkable natural richness, which makes it possible to adjust the knowledge of the atmospheric dynamics of the southern hemisphere through the SWW and its variability during the Holocene. This includes the migration between central-southern Patagonia and Antarctica, through local-scale studies, which, in turn, can be integrated at the regional level. The environmental variability in this region of the planet has been clearly recorded for the last 10,000 years and, apparently, more frequently towards the present.

CRediT authorship contribution statement

Ana María Borromei: Writing – review & editing, Writing – original draft, Methodology, Investigation, Funding acquisition, Formal analysis, Conceptualization. **Juan Federico Ponce:** Writing – review & editing, Writing – original draft, Methodology, Investigation, Funding acquisition, Formal analysis, Conceptualization. **Soledad Candel:** Writing – review & editing, Writing – original draft, Investigation, Formal analysis, Conceptualization. **Lorena Musotto:** Writing – review & editing, Writing – original draft, Investigation, Formal analysis. **Marilén Fernández:** Writing – original draft, Investigation, Funding acquisition, Formal analysis. **Cecilia Laprida:** Writing – review & editing, Writing – original draft, Investigation, Formal analysis. **Adriana Mehl:** Writing – original draft, Investigation, Formal analysis, Conceptualization. **Alejandro Montes:** Writing – review & editing, Writing – original draft, Investigation, Funding acquisition, Formal analysis, Conceptualization, Josefa Coronato, Writing – review & editing, Writing – original draft, Visualization, Methodology, Investigation, Funding acquisition, Conceptualization. **Cristina San Martín:** Writing – original draft, Investigation. **Adolfina Savoretti:** Writing – original draft, Investigation, Formal analysis. **Gabriela Cusminsky:** Writing – original draft, Investigation, Formal analysis, Conceptualization. **Sandra Gordillo:** Writing – original draft, Investigation, Funding acquisition, Formal analysis. **María Julia Orgeira:** Writing – original draft, Investigation. **Ramiro López:** Visualization. **Pamela Alli:** Writing – original draft. **Diego Quiroga:** Writing – original draft, Visualization.

Declaration of competing interest

The authors declare that they have no known competing financial interests or personal relationships that could have appeared to influence the work reported in this paper.

Data availability

Data will be made available on request.

Acknowledgments

The authors wish to thank the colleagues, students, and assistants who participated along the time in the different research projects from which the results integrated here were obtained. CONICET, ANPCYT, UBACYT financed various projects related to the previous works included and discussed here. The financial support to prepare this paper was obtained from PIP CONICET 405/17 to A. Coronato, PIP CONICET 112-201301-00323 to A. Borromei, PI 1590 FCNyCSCR-UNPSJB to A. Montes and from IDEAN-CONICET-UBA, Universidad Nacional del Comahue, Universidad Nacional de Córdoba, Universidad Nacional de La Pampa and Universidad de Buenos Aires. The farms María Behety, Flamencos, San Julio, Harberton, and Terra Australis company, among others, provided permits to work in their properties. The Río Grande Astronomical Station (EARG) provided assistance with the fieldwork logistics. Thanks to the reviewers for their valuable suggestions that helped to improve the manuscript.

8-References

- Aniya, M., 2013. Holocene glaciations of hielo patagónico (Patagonia icefield), south America: a brief review. *Geochim. J.* 47, 97–105.
- Arambarri, A.M., Gamundi, I.J., 1984. Micoflora de la hojarasca de *Nothofagus pumilio* y *N. obliqua* II. *Darwiniana* 25 (1–4), 255–265.
- Ariztegui, D., Anselmetti, F.S., Gilli, A., Waldmann, N., 2008. Late Pleistocene environmental changes in Patagonia and Tierra del Fuego: a limnogeological approach. In: Rabassa, J. (Ed.), *The Late Cenozoic of Patagonia and Tierra del Fuego*. Elsevier Science, London, pp. 241–253.
- Aubry, M.P., Head, M.J., Piller, W.E., Berggren, W.A., 2020. Subseries/subepochs approved as a formal rank in the international stratigraphic guide. *Episodes* 43 (4), 1041–1044. <https://doi.org/10.18814/epiugs/2020/020066>.
- Auer, V., 1958. The Pleistocene of fuego-patagonia. Part II: the history of flora and vegetation. In: *Annales Academiae Scientiarum Fenniae, Series A III, Geologica-Geographica*, 50. *Publicationes Instituti Geographicus Universitatis Helsingiensis*, Helsinki.
- Auer, V., 1959. The Pleistocene of fuego-patagonia. Part III: shoreline displacements. In: *Annales Academiae Scientiarum Fenniae, Series A III Geologica-Geographica*, 60. *Publicationes Instituti Geographicus Universitatis Helsingiensis*, Helsinki.
- Auer, V., 1974. The isorythmicity subsequent to the Fuego-Patagonian and Fennoscandian ocean level transgressions and recessions of the Last Glaciation. The significance of tephrochronology, C-14 dating and micropaleontology for Quaternary Research. In: *Annales Academiae Scie. Fenniae, Series A III, Geologica-Geographica*, vol. 115. *Publicationes Instituti Geographicus Universitatis Helsingiensis*, Helsinki, pp. 1–98.
- Bayer, S., Gordillo, S., Morsan, E., 2016. Late Quaternary faunal changes in northeastern Patagonia (Argentina) according to a dynamic mosaic of benthic habitats: taphonomic and paleoecological analyses of mollusk assemblages. *Ameghiniana* 53 (6), 655–674.
- Berman, A.L., Silvestri, G.E., Tonello, M.S., 2018. On the differences between Last Glacial Maximum and Mid-Holocene climates in southern South America simulated by PMIP3 models. *Quat. Sci. Rev.* 185, 113–121.
- Bernasconi, E., Mansilla, M., Cusminsky, G., 2018. Recent foraminifers from South Atlantic Ocean (39°–41° S and 59°–62° W) used as indicators of different water masses. *J. Foraminifer. Res.* 48 (3), 201–222.
- Bernasconi, E., Candel, M.S., Borromei, A.M., 2021. Palaeoenvironmental Changes Based on Foraminifera during the Late Holocene at the Beagle Channel, Argentina. *Anais da Academia Brasileira de Ciências* (in press).
- Björck, S., Rundgren, M., Ljung, K., Unkel, I., Wallin, A., 2012. Multi-proxy analyses of a peat bog on Isla de los Estados, easternmost Tierra del Fuego: a unique record of the variable Southern Hemisphere Westerlies since the last deglaciation. *Quat. Sci. Rev.* 42, 1–14.
- Björck, S., Lambeck, K., Möller, P., Waldmann, N., Bennike, O., Jiang, H., Li, D., Sandgren, P., Nielsen, A.B., Porter, Ch., 2021. Relative sea level changes and glacio-isostatic modelling in the Beagle Channel, Tierra del Fuego, Chile: glacial and tectonic implications. *Quat. Sci. Rev.* 251, 106–657.
- Borromei, A.M., Quattrocchio, M., 2007. Holocene sea-level change and marine palynology of the Beagle Channel, southern Tierra del Fuego, Argentina. *Ameghiniana* 41 (1), 161–171.
- Borromei, A.M., Coronato, A., Franzén, L., Ponce, J.F., López Sáez, J.A., Maidana, N., Rabassa, J., Candel, M.S., 2010. Multiproxy record of Holocene paleoenvironmental change, Tierra del Fuego, Argentina. *Palaeogeogr. Palaeoclimatol. Palaeoecol.* 286, 1–16.
- Borromei, A.M., Ponce, J.F., Coronato, A., Candel, M.S., Olivera, D., Okuda, M., 2014. Reconstrucción de la vegetación postglacial y su relación con el ascenso relativo del nivel del mar en el extremo SE del Canal Beagle, Tierra del Fuego. *Andean Geol.* 41 (2), 362–379.
- Borromei, A.M., Musotto, L.L., Coronato, A., Ponce, J.F., Pontevedra-Pombal, X., 2016. Postglacial vegetation and climate changes inferred from a peat pollen record in the Río Pipo valley, southern Tierra del Fuego. *Publicación Electrónica de la Asociación Paleontológica Argentina* 16 (2), 168–183.
- Borromei, Ana María, 1995. Análisis polínico de una turbera holocénica en el valle de Andorra, Tierra del Fuego, Argentina. *Revista Chilena de Historia Natural* 68, 311–319.
- Borromei, A.M., Candel, M.S., Musotto, L.L., Cusminsky, G., Martínez, M.A., Coviaga, C. A., Ponce, J.F., Coronato, A., 2018. Late Holocene wet/dry intervals from Fuegian steppe at Laguna Carmen, southern Argentina, based on a multiproxy record. *Palaeogeogr. Palaeoclimatol. Palaeoecol.* 499, 56–71.
- Bujalesky, G., 1997. Patrón espacial y dinámica de canales de sobrelevado de la costa atlántica septentrional de Tierra del Fuego. *Rev. Asoc. Geol. Argent.* 52, 257–274.
- Bujalesky, G., 1998. Holocene coastal evolution of Tierra del Fuego, Argentina. *Quat. S. Am. Antarct. Peninsula* 11, 247–282.
- Bujalesky, G., 2007. Coastal geomorphology and evolution of Tierra del Fuego (Southern Argentina). *Geol. Acta* 5, 337–362.
- Bujalesky, G., 2011. The Flood of the Beagle Channel (11,000 YR BP), Tierra del Fuego. *An. Inst. Patagonia* 39, 5–21.
- Bujalesky, G., Coronato, A., Isla, F.I., 2001. Ambientes glacifluviales y litorales cuaternarios de la región del río Chico, Tierra del Fuego, Argentina. *Rev. Asoc. Geol. Argent.* 56, 73–90.
- Bujalesky, G., Isla, F., Montes, A., 2021. Differential uplifting rates across the magellan fault: interactions between south American and Scotia plates. In: Acevedo, R.D. (Ed.), *Geological Resources of Tierra del Fuego*. Springer Geology, Cham, pp. 289–309.
- Candel, M.S., 2010. Cambios relativos del nivel del mar en el Canal Beagle, Tierra del Fuego (Cenozoico tardío), en base al análisis palinológico. Ph.D. thesis. Universidad Nacional del Sur.
- Candel, M.S., Borromei, A.M., 2013. Caracterización taxonómica y paleoecológica de la ingresión del Holoceno en el Canal Beagle (Tierra del Fuego) en base a las asociaciones de dinoquistes y otros palinomorfos acuáticos. *Rev. Bras. Palaontol.* 16, 245–262.
- Candel, M.S., Borromei, A.M., 2016. Palaeoenvironmental reconstruction of late Quaternary marine sequences, Tierra del Fuego (Argentina). *Publicación Electrónica de la Asociación Paleontológica Argentina* 16 (2), 184–201.
- Candel, M.S., Borromei, A.M., Martínez, M.A., Gordillo, S., Quattrocchio, M., Rabassa, J., 2009. Middle-Late Holocene palynology and marine mollusks from Archipiélago Cormoranes area, Beagle Channel, southern Tierra del Fuego, Argentina. *Palaeogeogr. Palaeoclimatol. Palaeoecol.* 273, 111–122.

- Candel, M.S., Martínez, M.A., Borromei, A.M., 2011. Palinología y palinofacies de una secuencia marina del Holoceno medio-tardío: Albufera Lanushuaia, Canal Beagle, Tierra del Fuego, Argentina. *Rev. Bras. Paleontol.* 14 (3), 297–310.
- Candel, M.S., Louwyne, S., Borromei, A.M., 2017. Reconstruction of the late Holocene paleoenvironment of the western Beagle Channel (Argentina) based on a palynological analysis. *Quat. Int.* 44 (PartA), 2–12.
- Candel, M.S., Borromei, A.M., Louwyne, S., 2018. Early to middle Holocene palaeoenvironmental reconstruction of the Beagle Channel (southernmost Argentina) based on terrestrial and marine palynomorphs. *Boreas* 47, 1072–1083.
- Candel, M.S., Díaz, P.E., Borromei, A.M., Fernández, M., Montes, A., Santiago, F.C., 2020. Multiproxy analysis of a Lateglacial-Holocene sedimentary section in the Fuegian steppe (northern Tierra del Fuego, Argentina): implications for coastal landscape evolution in relation to climatic variability and sea-level fluctuations. *Palaeogeogr. Palaeoclimatol. Palaeoecol.* 557, 109941 <https://doi.org/10.1016/j.palaeo.2020.109941>.
- Collantes, M.B., Anchorena, J., Cingolani, A.M., 1999. The steppes of Tierra del Fuego: floristic and growth form patterns controlled by soil fertility and moisture. *Plant Ecol.* 140, 61–75.
- Compagnucci, R.H., 2011. Atmospheric circulation over Patagonia from the Jurassic to present: a review through proxy data and climatic modelling scenarios. *Biol. J. Linn. Soc.* 103, 229–249.
- Coronato, A., 1994. Geomorfología Glacial de valles de los Andes Fueguinos y condicionantes ambientales para la ocupación humana. In: PHD Thesis. Universidad de Buenos Aires.
- Coronato, A., Meglioli, A., Rabassa, J., 2004. Glaciations in the Magellan Straits and Tierra del Fuego, Southernmost South America. In: Ehlers, J., Gibbard, P. (Eds.), Quaternary Glaciations – Extent and Chronology. Part III América del Sur, Asia, África, Australasia, Antártida. Developments in Quaternary Sciences. Elsevier Publishers, Amsterdam, pp. 45–48.
- Coronato, A., Coronato, F., Mazzoni, E., Vázquez, M., 2008. Physical Geography of Patagonia and Tierra del Fuego. In: Rabassa, J. (Ed.), Late Cenozoic of Patagonia and Tierra del Fuego, Development in Quaternary Sciences, vol. 11. Elsevier Publishers, Amsterdam, pp. 13–56.
- Coronato, A., Fanning, P., Salemme, M., Oría, J., Pickard, J., Ponce, J., 2011. Aeolian sequence and the archaeological record in the Fuegian steppe, Argentina. *Quat. Int.* 245, 122–135.
- Coronato, A., Llopiz, S., Ponce, J.F., Villarreal, M.L., López, R., 2012. Paleorelieves lacustres en la estepa fueguina: ¿expansión-retracción asociada a cambios ambientales durante el Holoceno?. In: V Congreso Argentino de Cuaternario y Geomorfología, Actas de Resúmenes UniRío Editora, Río Cuarto.
- Coronato, A., Ponce, J.F., Quiroga, D., Gogorza, C., 2017. Caracterización geológica y geomorfológica de la cuenca de la laguna Carmen (Estepa Fueguina, Argentina) y su registro sedimentario durante el Holoceno tardío. *Rev. Asoc. Geol. Argent.* 74 (2), 263–273.
- Coronato, A., Salemme, M., Oría, J., Mari, F., López, R., 2021. Perched dunes in the fuegian steppe, southern Argentina: archeological reservoirs of Holocene information. In: Collantes, M., Perucca, L., Niz, A., Rabassa, J. (Eds.), Advances in Geomorphology and Quaternary Studies in Argentina, Springer Earth System Sciences. Springer, Cham, pp. 58–91.
- Davies, B., Glasser, N., 2012. Accelerating shrinkage of patagonian glaciers from the little ice age (~AD 1870) to 2011. *J. Glaciol.* 58 (212), 1063–1084. <https://doi.org/10.3189/2012JoG12J026>.
- Díaz Balocchi, L., Ponce, J.F., Tripaldi, A., Magneres, I., 2020. Geomorphology of the northeastern extreme of Isla Grande de Tierra del Fuego, Argentina. *J. Maps* 16 (2), 512–523.
- Echeverría, M.E., Bamonte, F.P., Marcos, M.A., Sottile, G.D., Mancini, M.V., 2017. Palaeohydric balance variations in eastern Andean environments in southern Patagonia (48°–52.5° S): major trends and forcings during the last ca. 8000 cal yrs BP. *Rev. Palaeobot. Palynol.* 246, 242–250.
- Esper, J., Cook, E.R., Schweingruber, F.H., 2002. Low-frequency signals in long tree-ring chronologies for reconstructing past temperature variability. *Science* 295, 2250–2253.
- Etourneau, J., Collins, L.G., Willmott, V., Kim, J.H., Barbara, L., Leventer, A., Schouten, S., Sinninghe Damst, J.S., Bianchini, A., Klein, V., Crosta, X., Mass, G., 2013. Holocene climate variations in the western Antarctic Peninsula: evidence for sea ice extent predominantly controlled by insolation and ENSO variability changes. *Clim. Past* 9, 1431–1446.
- Falaschi, D., Bravo, C., Masiokas, M., Villalba, R., Rivera, A., 2013. First glacier inventory and recent changes in glacier area in the monte san lorenzo region (47°S), southern patagonian Andes, south America. *Artic, Antarctic Alpine Res.* 45 (1), 19–28.
- Falaschi, D., Lenzano, M.G., Villalba, R., Bolch, T., Rivera, A., Lo Vecchio, A., 2019. Six decade (1958–2018) of geodetic glacier mass balance in monte san lorenzo, patagonian Andes. *Front. Earth Sci.* 7 <https://doi.org/10.3389/feart.2019.00326>. Article 236.
- Favier Dubois, C., 2003. Late Holocene climatic fluctuations and soil genesis in southern Patagonia: effects on the archaeological record. *J. Archaeol. Sci.* 30, 1657–1664.
- Favier-Dubois, C., 2007. Soil genesis related to medieval climatic fluctuations in southern Patagonia and Tierra del Fuego (Argentina): chronological and paleoclimatic considerations. *Quat. Int.* 162–163, 158–165.
- Fernández, M., Maidana, N., Rabassa, J., 2012. Palaeoenvironmental conditions during the Middle Holocene at Isla de los Estados (Staten Island, Tierra del Fuego, 54 S, Argentina) and their influence on the possibilities for human exploration. *Quat. Int.* 256, 78–87.
- Fernández, M., Björck, S., Wohlfarth, B., Maidana, N.I., Unkel, I., Van der Putten, N., 2013. Diatom assemblage changes in lacustrine sediments from Isla de los Estados, southernmost South America, in response to shifts in the southwesterly wind belt during the last deglaciation. *J. Paleolimnol.* 50, 433–446.
- Fernández, M., Candel, S., Ponce, J.P., Rabassa, J., 2014. Primeras evidencias de la transgresión marina del Holoceno medio en Isla de los Estados (Tierra del Fuego) a partir de estudios de palinomorfos acuáticos y diatomeas. XIX Congreso Geológico Argentino, Córdoba.
- Fernández, M., Ponce, J.F., Ramón Mercau, J., Laprida, C., Maidana, N.I., Quiroga, D., Magneres, I., Coronato, A.M.J., 2020. Paleolimnological response to climate variability during Late Glacial and Holocene times recorded in shallow lake Arturo, Fuegian steppe (Southern South America). *Palaeogeogr. Palaeoclimatol. Palaeoecol.* 550, 109737.
- Fontana, S.L., Bennett, K.D., 2012. Postglacial vegetation dynamics of western Tierra del Fuego. *Holocene* 22, 1–337. –1.350.
- Franco, N.V., Brook, G., Mancini, M.V., Vetrisano, L., 2016. Change in lithic technology and environment in southern continental Patagonia: the Chico and Santa Cruz rivers basins. *Quat. Int.* 422, 57–65.
- Frenguelli, J., 1924a. Diatomas de la Tierra del Fuego. *An. Soc. Cient. Argent.* 96, 225–263.
- Frenguelli, J., 1924b. Diatomas de la Tierra del Fuego. *An. Soc. Cient. Argent.* 97, 87–118.
- Gelorini, V., Verbeken, A., van Geel, B., Cocquyt, C., Verschuren, D., 2011. Modern nonpollen palynomorph (NPP) diversity in East African lake sediments. *Rev. Palaeobot. Palynol.* 164, 143–173.
- Glasser, N.F., Harrison, S., Winchester, V., Aniya, M., 2004. Late Pleistocene and Holocene paleoclimate and glacier fluctuations in Patagonia. *Global Planet. Change* 43, 79–101.
- Godeas, A.M., Aramburre, A.M., 2007. Hifomicetes lignícolas de Tierra del Fuego (Fungi, Fungi Imperfici, Hyphomycetales). *Bol. Soc. Argent. Bot.* 42, 59–69.
- Gordillo, S., 1999. Holocene molluscan assemblages in the magellan region. *Sci. Mar.* 63 (Suppl. 1), 15–22.
- Gordillo, S., Bujalesky, G.G., Pirazzoli, P.A., Rabassa, J.O., Saliége, J.F., 1992. Holocene raised beaches along the northern coast of the Beagle Channel, Tierra del Fuego, Argentina. *Palaeogeogr. Palaeoclimatol. Palaeoecol.* 99 (41), 54.
- Gordillo, S., Coronato, A., Rabassa, J., 1993. Late Quaternary evolution of subantarctic paleofjord, Tierra del Fuego. *Quat. Sci. Rev.* 12, 889–897.
- Gordillo, S., Coronato, A., Rabassa, J., 2008. Paleoecology and paleobiogeographic patterns of mid-Holocene mollusks from the Beagle Channel (southern Tierra del Fuego, Argentina). *Rev. Geol. Chile* 35, 321–333.
- Gordillo, S., Bernasconi, E., Cusminsky, G., Coronato, A., Rabassa, J., 2013. Late Quaternary environmental changes in southernmost South America reflected in marine calcareous macro-and-microfossils. *Quat. Int.* 305, 149–162.
- Gordillo, S., Bayer, M.S., Boretto, G., Charó, M., 2014. Mollusk Shells as Bio-Geo-Archives: Evaluating Environmental Changes during the Quaternary. Springer Briefs in Earth System Sciences, South America and the Southern Hemisphere, Springer, Cham.
- Gordillo, S., Brey, T., Beyer, K., Lomovasky, B., 2015. Climatic and environmental changes during the middle to late Holocene in southern South America: a sclerochronological approach using the bivalve *Retrotapes exalbidus* (Dillwyn) from the Beagle Channel. *Quat. Int.* 377, 83–90.
- Grill, S., Borromei, A.M., Quattrochio, M., Coronato, A., Bujalesky, G., Rabassa, J., 2002. Palynological and sedimentological analysis of Recent sediments from Río Varela, Beagle Channel, Tierra del Fuego, Argentina. *Rev. Espanola Micropaleontol.* 34 (2), 145–161.
- Grove, J., Switsur, R., 1994. Glacial geological evidence for the medieval warm period. *Climatic Change* 26, 143–169.(h) Camargo, S., Pacheco, J., 2009. El retroceso del Glaciar Vinciguerra como respuesta al cambio climático en los Andes de Tierra del Fuego, Argentina. In: Arena, López, y Ramírez Cadena, C.D. (Eds.), Glaciaciones, nieves y hielos de América Latina. Cambio climático y amenazas. Ingeominas, pp. 61–76.
- Haberzettl, T., Corbella, H., Fey, M., Janssen, S., Lücke, A., Mayr, C., Ohlendorf, C., Schabitz, F., Schleser, G., Wille, M., Wulf, S., Zolitschka, B., 2007. Lateglacial and Holocene wet-dry cycles in southern Patagonia: chronology, sedimentology and geochemistry of a lacustrine record from Laguna Potrok Aike, Argentina. *Holocene* 17 (3), 297–310.
- Hall, B.L., 2009. Holocene glacial history of Antarctica and the sub-Antarctic islands. *Quat. Sci. Rev.* 28, 2213–2230.
- Heaton, T.J., Keohler, P., Butzin, M., Bard, E., Reimer, R.W., Austin, W.E.N., Bronk Ramsey, C., Grootes, P.M., Hughen, K.A., Kromer, B., Reimer, P.J., Adkins, J., Burke, A., Cook, M.S., Olsen, J., Skinner, L.C., 2020. Marine20—the marine radiocarbon age calibration curve (0–55,000 cal BP). *Radiocarbon* 62, 779–820.
- Heusser, C.J., 1989. Climate and chronology of Antarctica and adjacent South America over the past 30,000 yr. *Palaeogeogr. Palaeoclimatol. Palaeoecol.* 76, 31–37.
- Heusser, C.J., 1998. Deglacial paleoclimate of the American sector of the Southern Ocean: late Glacial-Holocene records from the latitude of Canal Beagle (55°S), Argentine Tierra del Fuego. *Palaeogeogr. Palaeoclimatol. Palaeoecol.* 141, 277–301.
- Heusser, C.J., 2003. Ice age southern Andes – a chronicle of paleoecological events. In: Developments in Quaternary Science, vol. 3. Elsevier Publishers, Amsterdam.
- Hogg, A.G., Heaton, T.J., Hua, Q., Palmer, J.G., Turney, C.S.M., Southon, J., Bayliss, A., Blackwell, P., Boswijk, G., Bronk Ramsey, C., Pearson, C., Petley, F., Reimer, P., Reimer, R., Wacker, L., 2020. SHCal20 Southern Hemisphere calibration, 0–55,000 years cal BP. *Radiocarbon* 62. <https://doi.org/10.1017/RDC.2020.59>.
- Horta, L.R., Georgieff, S.M., Console Gonella, C.A., Busnelli, J., Ascherlo, C.A., 2011. ¿Registros de fluctuaciones paleobatimétricas del sistema lacustre Pueyrredón-Pasadas-Salitroso durante el Pleistoceno Tardío? – holoceno Temprano, noroeste de Santa Cruz, Argentina. Ser. Correlación Geol. 27 (2), 100–109.
- Hughes, M., Diaz, H., 1994. Was there a “medieval warm period” and if so, where and when. *Climatic Change* 26, 109–142.

- Irurzun, M.A., Orgeira, M.J., Gogorza, C.S.G., Sinito, A.M., Compagnucci, R., Zolitschka, B., 2014. Magnetic parameters and their paleoclimatic implications—the sediment record of the last 15 500 cal. BP from Laguna Potrok Aike (Argentina). *Geophys. J. Int.* 198 (2), 710–726.
- Isla, F.I., Bujalesky, G.G., 2000. Cannibalisation of Holocene gravel beach-ridge plains, northern Tierra del Fuego, Argentina. *Mar. Geol.* 170 (1–2), 105–122.
- Iturraspe, R., 2010. Las turberas de Tierra del Fuego y el cambio climático global. In: Fundación para la Conservación y el Uso Sustentable de los Humedales. Fundación Humedales-Wetlands International Buenos Aires.
- Iturraspe, R.J., 2011. Glaciares de Tierra del Fuego. Editorial Dunken, Buenos Aires.
- Kaplan, M.R., Schaefer, J.M., Strelin, J.A., Denton, G.H., Anderson, R.F., Vandergoes, M.J., Finkel, R.C., Schwartz, R., Travis, S.G., Garcia, J.L., Martini, M.A., Nielsen, S.H.H., 2016. Patagonian and southern South Atlantic view of Holocene climate. *Quat. Sci. Rev.* 141, 112–125.
- Kaplan, M., Strelin, J., Schaefer, J., Peltier, C., Martini, M., Flores, E., Winckler, G., Schwartz, R., 2020. Holocene glacier behavior around the northern Antarctic Peninsula and possible causes. *Earth Planet Sci. Lett.* 534, 116077 <https://doi.org/10.1016/j.epsl.2020.116077>.
- Kilian, R., Lamy, F., 2012. A review of Glacial and Holocene paleoclimate records from southernmost Patagonia (49°–55° S). *Quat. Sci. Rev.* 53, 1–23.
- Kilian, R., Hohner, M., Biester, H., Wallrabe-Adams, H.J., Stern, C.R., 2003. Holocene peat and lake sediment tephra record from the southernmost Chilean Andes (53°–55°S). *Rev. Geol. Chile* 30, 23–37.
- Krammer, K., Lange-Bertalot, H., 1986. Bacillariophyceae. 1. Teil: Naviculariaceae. *Süsswasserflora von Mitteleuropa*. S. Gustav Fisher Verlag, New York.
- Laprida, C., Orgeira, M.J., Fernández, M., Tófalo, R., Ramón Mercau, M.J., Silvestri, G., Berman, A.L., García Chápori, N., Plastani, M.S., Alonso, S., 2021. The role of southern Hemisphere Westerlies for Holocene hydroclimatic changes in Tierra del Fuego (Argentina) and the role of the South Westerly Winds. *Quat. Int.* 571, 11–25.
- Loisel, J., Yu, Z., 2013. Holocene peatland carbon dynamics in Patagonia. *Quat. Sci. Rev.* 69, 125–141.
- Mansilla, C.A., McCulloch, R.D., Morello, F., 2018. The vulnerability of the Nothofagus forest-steppe ecotone to climate change: palaeoecological evidence from Tierra del Fuego (~53°S). *Palaeogeogr. Palaeoclimatol. Palaeoecol.* 508, 59–70.
- Markgraf, V., 1980. New data on the late and postglacial vegetational history of La Misión, Tierra del Fuego, Argentina. IV Int. Palynol. Con. 3.
- Markgraf, V., 1993. Paleoenvironments and paleoclimates in Tierra del Fuego and southernmost Patagonia, South America. *Palaeogeogr. Palaeoclimatol. Palaeoecol.* 102, 351–355.
- Markgraf, V., Huber, U., 2010. Late and postglacial vegetation and fire history in Southern Patagonia and Tierra del Fuego. *Palaeogeogr. Palaeoclimatol. Palaeoecol.* 297, 351–366.
- Masiokas, M.H., Rivera, A., Espízua, L.E., Villalba, R., Delgado, S., Aravena, J.C., 2009a. Glacier fluctuations in extratropical South America during the past 1000 years. *Palaeogeogr. Palaeoclimatol. Palaeoecol.* 281 (3–4), 242–268. <https://doi.org/10.1016/j.palaeo.2009.08.006>.
- Masiokas, M.H., Luckman, B.H., Villalba, R., Delgado, S., Skvarca, P., Ripalta, A., 2009b. Little Ice Age fluctuations of small glaciers in the Monte Fitz Roy and Lago del Desierto areas, south Patagonian Andes, Argentina. *Palaeogeogr. Palaeoclimatol. Palaeoecol.* 281 (3–4), 351–362. <https://doi.org/10.1016/j.palaeo.2007.10.031>.
- Mauquoy, D., Blaauw, M., van Geel, B., Borromei, A., Quattrochio, M., Chambers, F., Possnert, G., 2004. Late-Holocene climatic changes in Tierra del Fuego based on multi-proxy analyses of peat deposits. *Quat. Res.* 61, 148–158.
- Maurer, M., Menounos, B., Clague, J., Osborn, J., 2012. Patagonian glacier advances in concert with those in western North America. In: 45th Annual Fall Meeting of the American Geophysical Union. American Geophysical Union.
- McCulloch, R., Fogwill, G., Sudgen, D., Bentley, M., Kubik, P., 2005. Chronology of the Last Glaciation in. *McCulloch, R.D., Mansilla, C.A., Morello, F., De Pol-Holz, R., San Román, M., Tisdall, E., Torres, J., 2019. Late glacial and Holocene landscape change and rapid climate and coastal impacts in the Canal Beagle, southernmost Patagonia. *J. Quat. Sci.* 1–11.*
- McCulloch, R.D., Blaikie, J., Jacob, B., Mansilla, C.A., Morello, F., De Pol-Holz, R., San Roman, M., Tisdall, E., Torres, J., 2020. Late glacial and Holocene climate variability, southernmost Patagonia. *Quat. Sci. Rev.* 229, 106–131.
- Meglioli, A., Evenson, E., Zeitler, P., Rabassa, J., 1990. Cronología relativa absoluta de los depósitos glaciarios de Tierra del Fuego, Argentina y Chile, vol. 2. XI Congreso Geológico Argentino. San Juan.
- Meier, W.J.-H., Grießinger, J., Hochreuther, P., Braun, M.H., 2018. An updated multi-temporal glacier inventory for the Patagonian Andes with changes between the Little Ice Age and 2016. *Front. Earth Sci.* 6, 62. <https://doi.org/10.3389/feart.2018.00062>.
- Menounos, B., Clague, J.J., Osborn, G., Davis, T.P., Ponce, F., Goehring, B., Maurer, M., Rabassa, J., Coronato, A., Marr, R., 2013. Latest Pleistocene and Holocene glacier fluctuations in Southernmost Tierra del Fuego, Argentina. *Quat. Sci. Rev.* 77, 70–79.
- Montes, A., 2015. Morfología y evolución de depósitos litorales del Holoceno en la zona del río Chico, Tierra del Fuego. PH.D. thesis. Universidad Nacional de la Patagonia San Juan Bosco.
- Montes, A., Martinioni, D., 2017. Geomorfología y paleoambientes holocenos de la costa atlántica de Tierra del Fuego entre el río Grande y el estrecho de Le Maire. In: Oría, J., Vázquez, M., Elkin, R. (Eds.), *Patrimonio a orillas del Mar*, Editorial Cultural Tierra del Fuego, Ushuaia.
- Montes, A., Bujalesky, G., Paredes, J., 2018. Geomorphology and internal architecture of Holocene sandy-gravel beach ridge plain and barrier spits at Río Chico area, Tierra del Fuego, Argentina. *J. S. Am. Earth Sci.* 84, 172–183.
- Montes, A., Santiago, F., Salemme, M., López, R., 2020. Late Pleistocene and Holocene geomorphologic evolution of Laguna Las Vueltas area, Tierra del Fuego (Argentina). *Andean Geol.* 47 (1), 61–76.
- Moore, D., 1983. Flora of Tierra del Fuego. Anthony Nelson Publisher, London.
- Moreno, P.I., Vilanova, I., Villa-Martínez, R., Garreaud, R.D., Rojas, M., De Pol-Holz, R., 2014. Southern annular mode-like changes in southwestern Patagonia at centennial timescales over the last three millennia. *Nat. Commun.* 5, 4375.
- Moreno, P.I., Vilanova, I., Villa-Martínez, R., Dunbar, R.B., Mucciarone, D.A., Kaplan, M.R., Garreaud, R.D., Rojas, M., Moy, C.M., De Pol-Holz, R., Lambert, F., 2018. Onset and evolution of southern annular mode-like changes at centennial timescale. *Sci. rep.* Nat. 8, 3458.
- Moreno, P., Henríquez, W., Pesce, O., Henríquez, C., Fletcher, M., Garreaud, R., Villa-Martínez, R., 2021. An early Holocene westerly minimum in the southern mid-latitudes. *Quat. Sci. Rev.* 251, 106730 <https://doi.org/10.1016/j.quascirev.2020.106730>.
- Mulvaney, R., Abram, N.J., Hindmarsh, R.C.A., Arrowsmith, C., Fleet, L., Triest, J., Sime, L.C., Alemany, O., Foord, S., 2012. Recent Antarctic Peninsula warming relative to Holocene climate and ice-shelf history. *Nature* 448, 141–144.
- Musotto, L.L., Borromei, A.M., Coronato, A., Menounos, B., Osborn, G., Marr, R., 2016. Late Pleistocene and Holocene paleoenvironmental changes in central Tierra del Fuego (~54°S) inferred from pollen analysis. *Veg. Hist. Archaeobotany* 25 (2), 117–130.
- Musotto, L.L., Bianchinotti, M.V., Borromei, A.M., 2013. Inferencias paleoecológicas a partir del análisis de microfósiles fúngicos en una turbera pleistoceno-holocena de Tierra del Fuego (Argentina). *Revista del Museo Argentino de Ciencias Naturales "Bernardino Rivadavia"* 15 (1), 89–98.
- Musotto, L.L., Borromei, A.M., Bianchinotti, M.V., Coronato, A., 2017a. Late Quaternary paleoenvironmental reconstruction of central Tierra del Fuego (Argentina) based on main fossil pollen and fungi. *Quat. Int.* 442, 13–25.
- Musotto, L.L., Borromei, A.M., Bianchinotti, M.V., Coronato, A., Menounos, B., Osborn, G., Marr, R., 2017b. Postglacial environments in the southern coast of Lago Fagnano, central Tierra del Fuego, Argentina, based on pollen and fungal microfossils analyses. *Rev. Palaeob. Palynol.* 238, 43–54.
- Musotto, L.L., Borromei, A.M., Candel, M.S., Mehli, A., Bianchinotti, M.V., Coronato, A., 2022. Middle to late Holocene environmental conditions inferred from paleosols at the perched dune in the Laguna Arturo, Fuegian steppe, southern Argentina. *Paleogeography, Paleoclimatology, Paleoecology* 588, 1–15. <https://doi.org/10.1016/j.palaeo.2021.110806>, 110806.
- Musotto, L.L., Candel, M.S., Borromei, A.M., Ponce, J.F., Bianchinotti, M.V., Coronato, A., 2018. La palinología como una herramienta para la caracterización de paleoambientes continentales y marinos del Cuaternario Tardío en el Archipiélago Fueguino. *Publicación Electrónica de la Asociación Paleontológica Argentina* 18 (2), 131–155. <https://doi.org/10.5710/PEAPA.16.05.2018.248>.
- Naranjo, J., Stern, C., 1998. Holocene explosive activity of the Hudson volcano, southern Andes. *Bull. Volcanol.* 59, 291–306.
- Obelic, B., Álvarez, A., Arguello, J., Piana, E., 1998. Determination of water paleotemperature in the Beagle Channel (Argentina) during the last 6000 yr through stable isotope composition of *Mytilus edulis* shells. *Quat. S. Am. Antarct. Peninsula* 11, 47–71.
- Olivero, E.B., Martinioni, D.R., 2001. A review of the geology of the argentinian fuegian Andes. *J. S. Am. Earth Sci.* 14 (2), 175–188.
- Orgeira, M.J., Vásquez, C.A., Coronato, A., Ponce, J.F., Moreto, A., Osterrieth, M., Egli, R., Onorato, R., 2012. Magnetic properties of Holocene edaphized silty aeolian sediments from Tierra del Fuego (Argentina). *Rev. Soc. Geol. Espana* 25 (1–2), 45–56.
- Pérez Alberti, A., Coronato, A., Costa Casais, M., Valcarcel Diaz, M., Rabassa, J., 2008. Wedge structures in Southernmost Argentina (Río Grande, Tierra del Fuego). In: *Abstract Volume, NICOP-Ninth International Conference on Permafrost*. Posdam.
- Perren, B., Hodgson, D.A., Roberts, S.J., Sime, L., Van Nieuwenhuyse, P., Verleyen, E., Vyverman, W., 2020. Southward migration of the Southern Hemisphere westerly winds corresponds with warming climate over centennial timescales. *Commun. Earth Environ.* 1, 58. <https://doi.org/10.1038/s43247-020-00059-6>.
- Planas, X., Ponsa, A., Coronato, A., Rabassa, J., 2002. Geomorphological evidence of different glacial stages in the Martial cirque, Fuegian Andes, southernmost South America. *Quat. Int.* 87 (1), 19–27.
- Ponce, J.F., Fernández, M., 2013. Climatic and Environmental History of Isla de los Estados, Argentina. Springer Briefs in Earth Systems Sciences. South America and the Southern Hemisphere, Springer, Cham.
- Ponce, J.F., Borromei, A.M., Rabassa, J., Martínez, O., 2011. Late quaternary paleoenvironmental change in western staatens island (54.5S, 64W), fuegian Archipelago. *Quat. Int.* 233, 89–100.
- Ponce, J.F., Menounos, B., Fernández, M., Schaefer, J., 2015. Chronology and Extent of Outermost Cirque Moraines in the Southernmost Fuegian Andes and Canadian Cordillera. *Resúmenes, 6º Congreso Argentino de Cuaternario y Geomorfología, Ushuaia*.
- Ponce, J.F., Borromei, A.M., Menounos, B., Rabassa, J., 2017. Late-Holocene and Little Ice Age paleoenvironmental change inferred from pollen analysis, Isla de los Estados, Argentina. *Quat. Int.* 442, 26–34.
- Ponce, J.F., Balocchi, L.D., López, R., San Martín, C., 2020. Caracterización geomorfológica y sedimentológica del campo de eskers de Estancia Harberton, costa norte del canal Beagle, Argentina. *Rev. Asoc. Geol. Argent.* 77 (1), 79–90.
- Porter, S., Stuiver, M., Heusser, C.J., 1984. Holocene sea-level changes along the strait of magellan and Beagle channel, southernmost south America. *Quat. Res.* 22, 59–67.
- Prémoli, A., Mathiasen, P., Kitzberger, T., 2010. Southernmost Nothofagus trees enduring ice ages: genetic evidence and ecological niche retrodiction reveal high

- latitude (54°S) glacial refugia. *Palaeogeogr. Palaeoclimatol. Palaeoecol.* 298, 247–256.
- Quade, J., Kaplan, M.R., 2017. Lake-level stratigraphy and geochronology revisited at Lago (Lake) Cardiel, Argentina, and changes in the Southern Hemispheric westerlies over the last 25 ka. *Quat. Sci. Rev.* 177, 173–188.
- Quiroga, D., Crosta, S., Coronato, A., 2017. Bloques erráticos en el interfluvio Chico-Grande: evidencias de englazamiento en la estepa fueguina. In: *Actas, XX Congreso Geológico Argentino. San Miguel de Tucumán, Argentina.*
- Rabassa, J., 2008. Late Cenozoic Glaciations in Patagonia and Tierra del Fuego. In: Rabassa, J. (Ed.), *Late Cenozoic of Patagonia and Tierra del Fuego, Development in Quaternary Sciences*, vol. 11. Elsevier Publishers, Amsterdam, pp. 151–204.
- Rabassa, J.O., Heusser, C., Stuckenrath, R., 1986. New Data on Holocene Sea Transgression in the Beagle Channel: Tierra del Fuego, Argentina. *Quat. S. Am. Antarct. Peninsula* 4, 291–309.
- Rabassa, J., Heusser, C.J., Rutter, N., 1990. Late-Glacial and Holocene of Tierra del Fuego, Argentina. *Quat. S. Am. Antarct. Peninsula* 7, 327–351.
- Rabassa, J., Coronato, A., Bujalesky, G., Roig, C., Salemma, M., Meglioli, A., Heuser, C., Gordillo, S., Borromei, A., Quattrochio, M., 2000. Quaternary of Tierra del Fuego, Southernmost South America: an updated review. *Quat. Int.* 68–71, 217–240.
- Rabassa, J., Coronato, A., Roig, C., Martínez, O., Serrat, D., 2003. Un bosque sumergido en bahía Sloggett, Tierra del Fuego, Argentina: evidencias de actividad geotectónica diferencial en el Holoceno tardío. In: Blanco Chao, R., López Bedoya, J., Pérez Alberti, A. (Eds.), *Procesos Geomorfológicos Y Evolución Costera*. Universidad de Santiago de Compostela, Santiago de Compostela, pp. 333–345.
- Rabassa, J., Coronato, A., Gordillo, S., Candel, M.S., Martínez, M.A., 2009a. Paleoenvironments littorales durante la Transgresión Marina Holocena en Bahía Lapataia, Canal Beagle, Parque Nacional Tierra del Fuego, Argentina. *Rev. Asoc. Geol. Argent.* 65 (4), 648–659.
- Rabassa, J., Coronato, A., Ponce, J.F., Seppälä, M., Lehtinen, M., Menounos, B., Clague, J., Osborn, G., 2009b. Record of Andean tephras in Tierra del Fuego, Argentina. IV Congreso Argentino de Cuaternario y Geomorfología, Asociación Argentina de Cuaternario y Geomorfología, La Plata.
- Ramos, L., Alperin, M., Schwab, A., Markgraf, V., Ariztegui, D., Cusminsky, G., 2019. Changes in ostracod assemblages and morphologies during lake level variations of Lago Cardiel (49° S), Patagonia, Argentina, over the last 15.6 ka. *Boreas* 149, 746–760. <https://doi.org/10.1111/bor.12371>.
- Renssen, H., Goosse, H., Fichefet, T., Masson-Delmotte, V., Koç, N., 2005. Holocene climate evolution in the high-latitude Southern Hemisphere simulated by a coupled atmosphere-sea ice-ocean-vegetation model. *Holocene* 15 (7), 951–964.
- Reynhout, S., Sagredo, E., Kaplan, M., Aravena, J.C., Martínez, M., Moreno, P., Rojas, M., Schwartz, R., Schaefer, J., 2019. Holocene glacier fluctuations in Patagonia are modulated by summer insolation intensity and paced by Southern Annular Mode-like variability. *Quat. Sci. Rev.* 220, 178–187. <https://doi.org/10.1016/j.quascirev.2019.05.029>.
- Reynhout, S., Kaplan, M., Sagredo, E., Aravena, J.C., Soteres, R., Schwartz, R., Schaefer, J., 2021. Holocene glacier history of northeastern Cordillera Darwin, southernmost South America (55°S). *Quat. Res.* 1–16. <https://doi.org/10.1017/qua.2021.45>.
- Rivera, A., Koppes, M., Bravo, C., Aravena, J.C., 2012. Little ice age advance and retreat of glaciar jorge montt, Chilean Patagonia. *Clim. Past* 8 (2), 403–414. <https://doi.org/10.5194/cp-8-403-2012>.
- Roig, C., 2004. Antecedentes sobre turberas en Tierra del Fuego. In: Blanco, D.E., de la Balze, V.M. (Eds.), *Los turbales de la Patagonia. Bases para su inventario y la conservación de su biodiversidad*. Wetlands International, Buenos Aires.
- Roig, F.A., Villalba, R., 2008. Understanding climate from Patagonian tree rings. In: Rabassa, J. (Ed.), *The Late Cenozoic of Patagonia and Tierra del Fuego, Developments in Quaternary Sciences, Series 11*. Elsevier Publishers, Amsterdam, pp. 411–436.
- San Martín, C.N., Ponce, J.F., Coronato, A., 2021a. Lakes and glaciers from fuegian Andes. Morphology, distribution and origin. In: Acevedo, R.D. (Ed.), *Geological Resources of Tierra del Fuego*. Springer Geology, Cham, pp. 173–188.
- San Martín, C.N., Ponce, J.F., Montes, A., Díaz Balocchi, L., Gorza, C., Coronato, A., 2021b. Proglacial landform assemblage in a rapidly retreating cirque glacier due to temperature increase since 1970, Fuegian Andes, Argentina. *Geomorphology* 390, 1–15. <https://doi.org/10.1016/j.geomorph.2021.107861>.
- Savoretti, A., 2018. Estudio de las briofitas de turberas de Tierra del Fuego (Argentina) desde el Último Máximo Glacial a la actualidad y su relación con las fluctuaciones climáticas y ambientales. Ph.D. Thesis. Universidad Nacional de La Plata.
- Savoretti, A., Fernández, D.A., Iglesias, A., Ponce, J.F., 2017. Propuesta metodológica para el estudio de macrorrestos de briofitas en turberas. *Bol. Soc. Argent. Bot.* 52 (2), 371–381.
- Schäbitz, F., Wille, M., Francois, J.P., Haberzettl, T., Quintana, F., Mayr, C., Lücke, A., Ohlendorf, C., Mancini, V., Paez, M.M., Prieto, A.R., Zolitschka, B., 2013. Reconstruction of palaeoprecipitation based on pollen transfer functions - the record of the last 16 ka from Laguna Potrok Aike, southern Patagonia. *Quat. Sci. Rev.* 71, 175–190.
- Schneider, C., Glaser, M., Kilian, R., Santana, A., Butorovic, N., Casassa, G., 2003. Weather observations across the southern Andes at 53S. *Phys. Geogr.* 24, 97–119.
- Shevenell, A.E., Ingalls, A.E., Domack, E.W., Kelly, C., 2011. Holocene Southern Ocean surface temperature variability west of the antarctic peninsula. *Nature* 470, 250–254.
- Stern, C., 2008. Holocene tephrochronology record of large explosive eruptions in the southernmost Patagonian Andes. *Bull. Volcanol.* 70, 435–454.
- Stine, S., Stine, M., 1990. A record from Lake Cardiel of climate change in southern South America. *Nature* 345, 705–707.
- Stoessel, L., Bogan, S., Martínez, G., Agnolin, F., 2008. Implicaciones paleoambientales de la presencia del género Ceratophys (Anura, Ceratophryinae) en contextos arqueológicos de la transición pampeano-patagónica en el Holoceno tardío (curso inferior del Río Colorado, Argentina). *Magallania* 36 (2), 195–203.
- Strelin, J., Iturraspe, R., 2007. Recent evolution and mass balance of cordon martial glaciers, Cordillera fuegian oriental. *Global Planet. Change* 59, 17–26.
- Strelin, J., Casassa, G., Rosqvist, G., Holmlund, P., 2001. Glaciaciones holocénicas en el valle del glaciar Ema, Monte Sarmiento, Tierra del Fuego. In: *Abstract symposium, Cambios vegetacionales y climáticos durante el último ciclo glacial-interglacial a lo largo de Chile continental. La Serena*.
- Strelin, J.A., Sone, T., Mori, J., Torielli, C.A., Nakamura, T., 2006. New data related to Holocene landform development and climatic change in James Ross island, antarctic peninsula. In: Fütterer, D.K., Damaske, D., Kleinschmidt, G., Miller, H., Tessensohn, F. (Eds.), *Antarctica: Contributions to Global Earth Sciences*. Springer Verlag, Berlin, pp. 453–458.
- Strelin, J., Casassa, G., Rosqvist, G., Holmlund, P., 2008. Holocene glaciations in the Ema Glacier Valley, Monte Sarmiento Massif, Tierra del Fuego. *Palaeogeogr. Palaeoclimatol. Palaeoecol.* 260, 299–314.
- Strelin, J., Kaplan, M., Vandergoes, M., Denton, G., Schaefer, J., 2014. Holocene glacier history of the Lago Argentino basin, southern patagonian icefield. *Quat. Sci. Rev.* 101, 124–145. <https://doi.org/10.1016/j.quascirev.2014.06.026>.
- Stuiver, M., Reimer, P.J., 1993. Extended ^{14}C data base and revised CALIB 3.0 14C age calibration program. *Radiocarbon* 35, 215–230.
- Torres Carbonell, P.J., Dimieri, L.V., Olivero, E.B., 2013. Evaluation of strain and structural style variations along the strike of the Fuegian thrust-fold belt front, Argentina. *Andean Geol.* 40 (3), 438–457. <https://doi.org/10.5027/andgeoV40n3-a03>.
- Tuhkanen, S., 1992. The climate of Tierra del Fuego from a vegetation geographical point of view and its ecoclimatic counterparts elsewhere. *Acta Bot. Fennica* 145, 1–64.
- Unkel, I., Björck, S., Wohlfarth, B., 2008. Deglacial environmental changes on Isla de los Estados (54°S), southeastern Tierra del Fuego. *Quat. Sci. Rev.* 27, 1541–1554.
- Unkel, I., Fernández, M., Björck, S., Kjung, K., Wohlfarth, B., 2010. Records of environmental changes during the Holocene from Isla de los Estados (54° S), southeastern Tierra del Fuego. *Global Planet. Change* 74, 99–113.
- Vanneste, H., De Vleeschouwer, F., Martinez-Cortizas, A., von Scheffer, C., Piotrowska, N., Coronato, A., Le Roux, A., 2015. Late-glacial elevated dust deposition linked to westerly wind shifts in southern South America. *Nat. Sci. Rep.* 5, 1–10.
- Villas, F., Arche, A., Ferrero, M., Isla, F., 1999. Subantarctic macrotidal flats, cheniers and beaches in san sebastian bay, Tierra del Fuego, Argentina. *Mar. Geol.* 160 (3–4), 301–326.
- Villa-Martínez, R.P., Moreno, P.I., 2007. Pollen evidence for variations in the southern margin of the westerly winds in SW Patagonia over the last 12,600 years. *Quat. Res.* 68, 400–409.
- Villarreal, M.L., Coronato, A., 2017. Characteristics and nature of pans in the semiarid temperate-cold steppe of Tierra del Fuego. In: Rabassa, J. (Ed.), *Advances in Geomorphology and Quaternary Studies in Argentina. Selected Papers of the VI Argentine Congress of Geomorphology and Quaternary Studies*. Springer Verlag, The Netherlands, pp. 203–224.
- Villarreal, M.L., Coronato, A., Mazzoni, E., López, R., 2014. Mantos eólicos y lagunas semipermanentes de la estepa fueguina (53°S), Argentina. *Revista de la Sociedad Espanola de Geología* 27 (2), 81–96.
- Waelbroeck, C., Skinner, L.C., Labeyrie, L., Duplessy, J.-C., Michel, E., Vazquez Riveiros, N., Gherardi, J.-M., Dewilde, F., 2011. The timing of deglacial circulation changes in the Atlantic. *Paleoceanography* 26, 3213. <https://doi.org/10.1029/2010PA002007>.
- Waldmann, N., Ariztegui, D., Anselmetti, F., Coronato, A., Austin-Jr. J., 2010. Geophysical evidence of multiple glacier advances in Lago Fagnano (54°S), southernmost Patagonia. *Quat. Sci. Rev.* 29 (9–10), 1188–1200.
- Waldmann, N., Borromei, A.M., Recasens, C., Olivera, D., Martínez, M.A., Maidana, N.I., Ariztegui, D., Austin Jr., J.A., Anselmetti, F.S., Moy, C.M., 2014. Integrated reconstruction of Holocene millennial-scale environmental changes in Tierra del Fuego, southernmost South America. *Palaeogeogr. Palaeoclimatol. Palaeoecol.* 399, 294–309.
- Walker, M., Head, M.J., Berkelhammer, M., Björck, S., Cheng, H., Cwynar, L., Fisher, D., Gkinis, V., Long, A., Lowe, J., Newnham, R., Rasmussen, S.O., Weiss, H., 2020. Formal ratification of the subdivision of the Holocene series/epoch (quaternary system/period): two new global boundary stratotype sections and points (GSSPs) and three new stages/subseries. *Episodes* 41 (4), 213–223.
- Wastegård, A., Veres, D., Kliem, P., Hahn, A., Ohlendorf, C., Zolitschka, B., The PASADO Science Team, 2013. Towards a late Quaternary tephrochronological framework for the southernmost part of South America e the Laguna Potrok Aike tephra record. *Quat. Sci. Rev.* 71, 81–90.
- Whatley, R.C., Cusminsky, G., 2002. Upper pliocene ostracoda from the burdwood bank, SW atlantic. *Rev. Espanola Micropaleontol.* 34 (1), 53–80.
- Whitlock, C., Moreno, P., Bartlein, P., 2007. Climatic controls of Holocene fire patterns in southern South America. *Quat. Res.* 68, 28–36.
- Xia, Z., Yu, Z., Loisel, J., 2018. Centennial-scale dynamics of the southern hemisphere westerly winds across the drake passage over the past two millennia. *Geol.* 46, 855–858.
- Zangrandino, A.F., Ponce, J.F., Martinoli, M.P., Montes, A., Piana, E., Vanella, F., 2016. Palaeogeographic changes drove prehistoric fishing practices in the Cambaceres Bay (Tierra del Fuego, Argentina) during the middle and late Holocene. *Environ. Archaeol.* 21 (2), 182–192.